

NASA MEMO 10-7-58A

C. 230

LOAN COPY: RET  
AFWL (WLL  
KIRTLAND AFB,

0063050



TECH LIBRARY KAFB, NM

NASA MEMO 10-7-58A

# NASA

## MEMORANDUM

AN ANALOG COMPUTER STUDY OF THE EFFECTIVENESS  
OF INTERCEPTOR COMMANDS DERIVED FROM  
A PREDICTION EQUATION OF  
SECOND ORDER

By Brian F. Doolin and John D. McLean

Ames Research Center  
Moffett Field, Calif.

This material contains information affecting the National Defense of the United States within the meaning of the espionage laws, Title 18, U.S.C., Secs. 793 and 794, the transmission or revelation of which in any manner to an unauthorized person is prohibited by law.

### NATIONAL AERONAUTICS AND SPACE ADMINISTRATION

WASHINGTON

November 1958

Classification canceled & changed to *Unclassified*  
by authority of *Mr. A. J. Clark, Chief, Policy, Plans, & Insp. Div.*  
Name and grade of official authorizing change  
*A. J. Clark*  
Date  
*22 Jan 68*

880 2016782 230

2 clds removed 20 Jan 64 fa

TECH LIBRARY KAFB, NM



0063050



NATIONAL AERONAUTICS AND SPACE ADMINISTRATION

MEMORANDUM 10-7-58A

AN ANALOG COMPUTER STUDY OF THE EFFECTIVENESS  
OF INTERCEPTOR COMMANDS DERIVED FROM  
A PREDICTION EQUATION OF  
SECOND ORDER\*

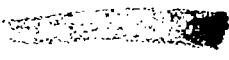
By Brian F. Doolin and John D. McLean

SUMMARY

The present report contains an attempt to improve the accuracy of an automatic interceptor flying a lead-collision course against a maneuvering target. For this improvement, the prediction equations that provide the interceptor's guidance were modified by incorporating terms of second order to predict the future location of a steadily maneuvering target. The interceptor commands derived from the second-order prediction equations allow the interceptor to fly a straight line course against a target flying with constant acceleration. The stability of the system is studied by means of an analog computer. The system accuracy was evaluated in terms of rocket miss and is compared on this basis with the performance of an interceptor with commands derived from a first-order prediction scheme. The comparison covers cases of unlimited and limited interceptor acceleration capability, constant and pulse acceleration target maneuvers, and variations in rocket speed.

INTRODUCTION

The present report is part of a flight and analog computer study of the final attack phase of automatic interception currently being conducted at the Ames Aeronautical Laboratory of the NACA. The initial work (ref. 1) concerned improvements in tracking accuracy and system stability of an interceptor flying a pursuit course. The work was continued in references 2 to 4, where improvements in system stability of an interceptor flying a lead-collision course against a nonmaneuvering target were reported.



SWC 8 C16 733 / 230

In a pursuit course, where an airplane tries to keep fixed guns pointed at a target for a protracted period of time, the system accuracy can be described in terms of the tracking accuracy of the interceptor. In a collision course, whether the interceptor's rockets hit or miss the target depends on the interceptor's heading and position at the single instant of firing, and the tracking accuracy at times other than firing time is much less important than it is in a pursuit course. However, although the tracking accuracy requirements of a rocket-firing interceptor on a collision course are low throughout most of an attack, the geometry computing accuracy requirements are high.

The components of a predicted miss are calculated from measured and computed geometric quantities. The computation is done by an attack computer which takes into account the present range and bearing of the target from the attacker, and how the range and bearing change with time. On the basis of this information and the knowledge of the distance and direction that the rockets will travel between the time they are fired and the time they should hit the target, the computer predicts by how much the rockets will miss the target. This predicted miss is converted into commands for the autopilot so to modify the heading of the airplane as to reduce the predicted miss to zero.

Since the actual, not predicted, rocket miss is the desired criterion, the accuracy of a system depends not only on how well the airplane follows its commands, but also on the quality of prediction. Here the quality of prediction refers to the sort of assumptions underlying its computation. In current fire-control systems, for instance, first-order prediction is used; that is, the miss is predicted on the assumption that the target will continue to maintain its present heading until impact time. If the target maneuvers, the rockets actually will miss the target even though the airplane is flying so as to keep the predicted miss zero. It is clear that improvement in radar and control system dynamics will not substantially change this result. A modification must be made to the prediction.

Modifying the prediction equation has not been the usual method adopted in designing interceptors for use against maneuvering targets. Since in first-order prediction a steady prediction lag is introduced by a steadily maneuvering target, the control systems approach has suggested that various amounts of integration be added to the autopilot commands. Experience, however, indicates that the addition of even varying amounts of integration decreases the interceptor system stability without satisfactorily improving the chances of hitting the target. Another method of reducing the steady error is to attempt input differentiation (e.g., see ref. 5) which can be applied successfully in pursuit-course problems where similar final geometry recurs from run to run, and the problem depends much less on time. This method, however, will not be successful when applied to a collision course unless the system gains are scheduled in a rational manner.

The simplest way to schedule the gains is to determine their dependence on the geometry of the particular attack. But the airborne determination of this dependence is just what is accomplished in the non-maneuvering case by the first-order prediction of miss. In the same way, a higher order of prediction can be made in the computation of miss that will take into account target maneuvers with reasonable success.

The present report summarizes some work done along these lines. A second-order equation of prediction is derived, and autopilot command equations are obtained from it. The characteristics of the resulting path of the interceptor (which is a straight line, regardless of the target acceleration, as long as it is constant) are compared with those of the path of the interceptor resulting from first-order prediction. The accuracy of two interceptor systems which differ only in their prediction and command equations is compared on the basis of "actual" miss by results of analog simulation. It is shown that, in contrast to the system under first-order guidance, the second-order system can be designed to perform successfully against targets in steady  $g$  turning maneuvers. Comparisons between first- and second-order predictions also are made to show the effect of limiting the attacker's maneuverability, and the effect of increasing the average speed of the attacker's armament.

The effects of additive input noise on the operation of the system have been ignored in this study. The present report primarily specifies the geometric dependence of the various terms of the attack computation, a dependence that will be common to all systems that try to accomplish the same task. Furthermore, it seems desirable to know whether or not a conceptual scheme will work and what are its inherent limitations apart from considerations of noise before optimization of a system is attempted. The answers to these questions can be ascertained only by such a study as is contained herein.

#### NOTATION

A	azimuth position angle between radar antenna and airplane (sketch (b)), radians
a,e,t	as superscripts or subscripts either differentiate between attacker, earth, or target coordinate systems or distinguish an attacker property from that of the target (as $V_a$ is attacker speed)
E	elevation position angle between radar antenna and airplane (sketch (b)), radians
F	distance traveled by the rocket relative to the attacker, ft

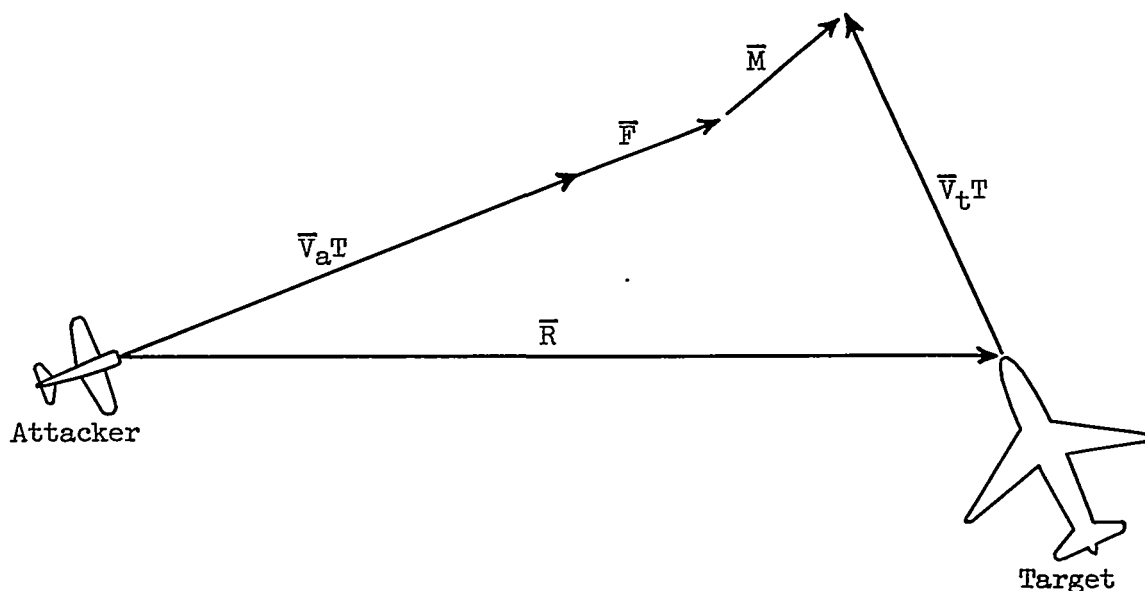
$g$	32.2 ft/sec <sup>2</sup>
$M$	miss, or distance between rocket and target at impact time, ft
$p, q, r$	angular velocity components of the airplane, radians/sec
$R$	present distance between target and attacker, ft
$s$	Laplace transform variable, 1/sec
$T$	time-to-go, duration of time from the present until impact time, sec
$t_f$	rocket travel time or time of firing, sec
$t_m$	time between the beginning of a target maneuver and impact time, sec
$V$	speed of attacker or target, ft/sec
$x, y$	position parameters of attacker or target in an earth reference system (sketch (c)), ft
$\alpha$	angle of attack of attacker airplane, radians
$\gamma$	attacker's velocity direction angle with respect to an earth reference (sketch (c)), radians
$\Delta t$	duration of acceleration pulse of target maneuver, sec
$\theta$	target velocity direction angle with respect to an earth reference (sketch (c)), radians
$\xi$	heading angle of radar antenna with respect to an earth reference (sketch (c)), radians
$\Omega$	rate of rotation of radar antenna coordinates, radians/sec
$1, 2, 3$	labels of any right-hand triad of unit vectors (as subscripts, the components of a vector associated with the pertinent unit vectors)
$(\vec{\quad})$	vector quantity

#### ANALYSIS

The simulation described in reference 2 was used in analog computer runs of the F-86D control-surface tie-in (CSTI) system against a target

executing steady  $g$  maneuvers in elevation. The runs indicated that large misses could be expected in attacking a target so maneuvering. Furthermore, it was apparent that the dynamics of the radar and the interceptor control system, if modified according to references 2 and 4, had relatively little effect on the magnitude of the misses which was due fundamentally to improper prediction in the attack computer. To improve these results, new second-order prediction equations were derived which reduce to the previous commands when the target makes no maneuver, but which enable the attacker to fly an effectively straight-line interception against a target in a steady  $g$  maneuver.

The meaning of the old prediction equations can be understood after inspection of sketch (a).



Sketch (a)

The quantities  $\bar{V}_a$  and  $\bar{V}_t$  represent the velocities of the attacker and target. The distance relative to the attacker travelled by a rocket is designated by  $\bar{F}$ . The relative position of the target from the attacker at any time is represented by  $\bar{R}$ . If the attacker and target each fly in a straight line, then in a time  $T$ , they travel a distance  $\bar{V}_a T$  and  $\bar{V}_t T$ , respectively. From the diagram, then  $\bar{V}_a T + \bar{F} + \bar{M} = \bar{R} + \bar{V}_t T$ , where  $\bar{M}$ , the miss, closes the vector polygon. Taking  $\bar{R} = \bar{V}_t T - \bar{V}_a T$ , one can write the equation  $\bar{M} + \bar{F} = \bar{R} + T\bar{R}$ .

The new prediction equations were derived after it was recognized that the miss equations mechanized in the present E-4 system can be considered a Taylor's expansion of the separation of the target and the interceptor around impact time. Second-order prediction equations are obtained simply

by incorporating a term of higher order in time-to-go,  $T$ . Instead of  $\bar{M} + \bar{F} = \bar{R} + T\dot{\bar{R}}$ , the equation becomes  $\bar{M} + \bar{F} = \bar{R} + T\dot{\bar{R}} + (T^2/2)\ddot{\bar{R}}$ . The first and second rates of range of target from attacker are represented by  $\dot{\bar{R}}$  and  $\ddot{\bar{R}}$ . The quantity  $T$ , the time-to-go, is the length of time from "now" until rocket impact.

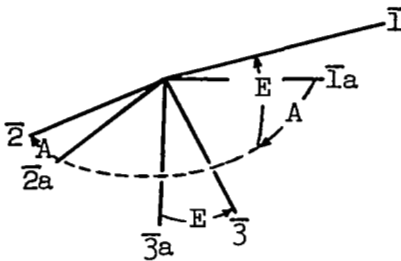
The new equation, when expressed in radar coordinates, is given by the following set of equations which are derived in appendix A.

$$M_1 = R - F \cos A \cos E + T \left( 1 + \frac{T}{2} \frac{\partial}{\partial t} \right) \dot{R} - \frac{T^2}{2} R(\Omega_2^2 + \Omega_3^2)$$

$$M_2 = F \sin A + \frac{T}{R} \left( 1 + \frac{T}{2} \frac{\partial}{\partial t} \right) R^2 \Omega_3 + \frac{T^2}{2} R \Omega_1 \Omega_2$$

$$-M_3 = F \cos A \sin E + \frac{T}{R} \left( 1 + \frac{T}{2} \frac{\partial}{\partial t} \right) R^2 \Omega_2 - \frac{T^2}{2} R \Omega_1 \Omega_3$$

The relationship between airframe and radar coordinates is indicated in sketch (b). The radar coordinate system, with unit vectors  $\bar{1}$ ,  $\bar{2}$ ,  $\bar{3}$ , is obtained from the airplane coordinate system (with unit vectors  $\bar{1}a$ ,  $\bar{2}a$ ,  $\bar{3}a$ ) by first rotating through the angle  $A$  about the  $\bar{3}a$  direction, then by rotating through the angle  $E$  about the  $\bar{2}$  direction.

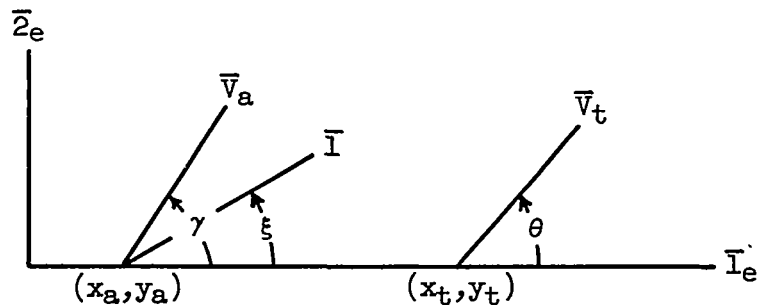


Sketch (b)

When all motion of the target and attacker is constrained to the same vertical plane, the azimuth component of miss,  $M_2$ , becomes zero. The other equations, the time and elevation components of miss, become

$$\left. \begin{aligned} M_1 &= R - F \cos E + T \left( 1 + \frac{T}{2} \frac{\partial}{\partial t} \right) \dot{R} - \frac{T^2}{2} R \Omega_2^2 \\ -M_3 &= F \sin E + \frac{T}{R} \left( 1 + \frac{T}{2} \frac{\partial}{\partial t} \right) R^2 \Omega_2 \end{aligned} \right\} \quad (1)$$

The significance of the various terms in equations (1) becomes more evident if the equations are expressed in a fixed coordinate system. With the definitions indicated in sketch (c),



Sketch (c)

the equations take the form

$$\left. \begin{aligned} M_{1e} &= -F \cos(\gamma - \xi) + x \cos \xi + y \sin \xi + T(\dot{x} \cos \xi + \dot{y} \sin \xi) + \\ &\quad \frac{T^2}{2} (\ddot{x} \cos \xi + \ddot{y} \sin \xi) \\ M_{2e} &= -F \sin(\gamma - \xi) + T(\dot{y} \cos \xi - \dot{x} \sin \xi) + \\ &\quad \frac{T^2}{2} (\ddot{y} \cos \xi - \ddot{x} \sin \xi) \end{aligned} \right\} (2)$$

where  $x = x_t - x_a$ ,  $y = y_t - y_a$ . The quantities  $V_a$ ,  $x_a$ ,  $y_a$ , and  $\gamma$  specify attacker speed, position, and heading. The quantities  $V_t$ ,  $x_t$ ,  $y_t$ , and  $\theta$  specify the target speed, position, and heading. The angle  $\xi$  specifies the heading of the radar which is mounted in the attacker and points toward the target. In the two-dimensional system under consideration, the system consists of the time-to-go, or simply, the time channel and the elevation channel. The time channel determines the proper instant at which to fire the rockets. The elevation channel determines the proper normal acceleration of the interceptor.

The miss equations (1) or (2) are not the appropriate expressions for use as commands to the airplane-autopilot system. Experience showed that a system using them as commands will be unstable. That portion of the relative acceleration due to the interceptor's own motion must be removed from them and the remaining signals used as the commands:



$$\begin{aligned}
 S_{1e} &= -F \cos(\gamma - \xi) + x \cos \xi + y \sin \xi + T(\dot{x} \cos \xi + \dot{y} \sin \xi) + \\
 &\quad \frac{T^2}{2} (\ddot{x}_t \cos \xi + \ddot{y}_t \sin \xi) \\
 &= M_{1e} + \frac{T^2}{2} (\ddot{x}_a \cos \xi + \ddot{y}_a \sin \xi) \\
 S_{2e} &= -F \sin(\gamma - \xi) + T(\dot{y} \cos \xi - \dot{x} \sin \xi) + \frac{T^2}{2} (\ddot{y}_t \cos \xi - \ddot{x}_t \sin \xi) \\
 &= M_{2e} + \frac{T^2}{2} (\ddot{y}_a \cos \xi - \ddot{x}_a \sin \xi)
 \end{aligned} \tag{3}$$

When written in the radar coordinates, these equations become

$$\begin{aligned}
 S_1 &= R - F \cos(E + \alpha) + TR + \frac{T^2}{2} [\ddot{R} - R\Omega^2 + V_a \dot{\gamma} \sin(E + \alpha)] \\
 S_2 &= F \sin(E + \alpha) + \frac{T}{R} \left( 1 + \frac{T}{2} \frac{\partial}{\partial t} \right) R^2 \Omega + \frac{T^2}{2} V_a \dot{\gamma} \cos(E + \alpha)
 \end{aligned} \tag{4}$$

When the interceptor performs according to these command equations, the miss equations are said to be nulled through the action of the "outer-loop geometry."

The results of numerical calculations made using equations (4) are shown in figures 1 and 2. They can be contrasted with the results computed with the same equations minus the terms in  $T^2$ , which are shown in figures 3 and 4. The computation assumes that the interceptor turns at a rate proportional to the elevation command without any dynamic effects; that is, the airplane-autopilot loop is assumed perfect. The speed of the interceptor,  $V_a$ , is taken to be 1,000 feet per second; that of the target, 800 feet per second. The target begins turning at the rate of 0.05 radian per second at the beginning of the calculation and is at that time 4,000 feet directly ahead of the interceptor. The value of  $F$  is 1,500 feet.

Figure 1 shows the path taken by the interceptor when flying against a target flying the course shown in the figure. The interceptor trajectory is nearly a straight line aimed at an impact point predicted immediately by its second-order attack computer. The path flown by the interceptor with a first-order attack computer is curved (fig. 3). In the latter case, since the impact point predicted at any time lies along the target's flight path at that instant, the impact point keeps changing its position. The interceptor, therefore, must maneuver continually.

In figures 1 and 3, the lines connecting the two flight paths represent the interceptor's line of sight to the target. The sequence

of lines in each figure provides a time history of the angle between this line and the interceptor's path. A comparison of the behavior of this lead angle in the two figures shows that it varies considerably in the case of second-order prediction, and remains nearly constant in the case of first-order prediction.

Figures 2 and 4 show the time histories of the terms of equations (4) from the computation. The terms of the first-order command system (fig. 4) are seen to be much smoother. The magnitude of the acceleration terms,

$$\frac{T^2}{2} (\ddot{R} - R\Omega^2 + V_a \dot{\gamma} \sin E) \text{ and } T \left( \frac{1}{R} \frac{\partial}{\partial t} R^2 \Omega + V_a \dot{\gamma} \cos E \right),$$

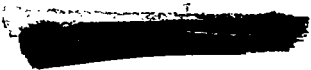
however, shows that they are not negligible, a fact graphically illustrated by difference in interceptor flight paths in figures 1 and 3. Figures 2(c) and (d) show the important influence of each of the components of the acceleration terms; none of them can be neglected without a serious modification of the shapes of the acceleration terms.

#### TEST EQUIPMENT AND PROCEDURE

In the previous section, a possible set of second-order command equations was obtained whose use should increase the effectiveness of an interceptor attacking a target which is turning at a steady rate. The analysis, however, neglected all those transient dynamic effects with which the designer of an actual system must cope. Since experience has indicated that results of studying a dynamic problem on an electronic analog computer agree quite well with results obtained in flight, and since the methods of mechanizing the prediction equation for an analog computer parallel those available to the designer of airborne hardware, it is useful to investigate the complete dynamic system on an electronic analog computer. The remainder of this report is concerned with an analog simulation to determine its stability and its effectiveness under varied conditions. The present section describes the simulation as set up on an Electronic Associates analog computer.

#### Simulation of Automatic Interceptors

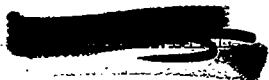
The simulation is a modification of the simulation of the F-86D CSTI system described in reference 2. The simplified block diagram (fig. 5), adapted from this reference, indicates that the system can be divided into five parts: radar, attack computer, attack coupler, airplane-autopilot loop, and geometry. The radar, being mounted on the interceptor and receiving reflected signals from the target, measures the range, range rate, position, and angular rate of the line of sight from the interceptor to the target and provides these data to the attack computer. The attack



computer is an analog device which operates on the radar-furnished quantities to compute a predicted value of miss by means of those miss-prediction equations described in the previous section on Analysis. It is the function of the attack coupler to process the predicted miss values provided by the computer into a form that the autopilot can use as commands to drive the airplane controls. It computes the normal acceleration required and bank-angle error of the interceptor. The airplane-autopilot loop, by properly reacting to the coupler commands, banks and accelerates to bring the predicted miss to zero. The box marked "geometry" in the diagram of figure 5, as far as the electronic analog computer is concerned, contains that assortment of operations on the motion of the two airplanes which provides the information on their absolute and relative positions relevant to the problem.

The present study required two basic changes in the simulation described in reference 2: the attack computer was expanded to include the operations necessary to obtain a second-order prediction of miss; and the geometry was diminished so as to fit the total problem on the two analog-computer consoles available. For geometric simplicity, the motions of the interceptor and target were confined to a single plane containing the vertical (i.e., a tail chase). Although this constraint is drastic, it does not invalidate the conclusions of the report for two reasons. In the first place, equations (1) of the previous section show what is needed analytically for the extension of the miss prediction to three dimensions, so that the extension may be made in a straightforward, though physically complicated, fashion. In the second place, preliminary unreported trials indicated that the most serious problems of stability peculiar to the second-order prediction were encountered during attack from the nose or tail of the target. Figure 6 illustrates in schematic form the geometry mechanized for the problem.

The geometric constraint decreased the requirements of the other four boxes shown in figure 5. The block diagram of figure 7 depicts the attack coupler and the airplane-autopilot loop. The constraint reduces the required channels from azimuth and elevation to elevation alone, as far as airplane performance is concerned. In the attack computer, only two channels are needed, the elevation channel, and the time channel. These channels are illustrated in figures 8 and 9. By comparison of the mechanization of first- and second-order prediction, these figures show the increase in operations needed for second-order miss prediction. The radar simulation can also be simplified. Since not only the geometric reduction but especially the improvements reported in reference 2 have removed the radar as a possible source of flight path instability, a radar transfer function of unity was used in the present work for both the first- and second-order systems.



## Simulation of Miss

The equations and method for obtaining the quantities from which the distance of miss was calculated are described in appendix B. A number of limitations on the actual motion of rockets was made which simplified the computation without invalidating the system performance comparisons described in this study. These limitations follow. A single average rocket is fired in any pass on the target, and flies in a straight line with a known average velocity along the direction tangent to the path of the interceptor at firing time. Its distance from the target is evaluated exactly 1.5 seconds after it has been fired. This distance is the value of miss used in this report.

## RESULTS AND DISCUSSION

The considerations in this section are divided into two parts. Into the first fall the considerations about mechanizing the prediction and command equations so as to insure stability and smoothness of the interceptor operation. The practical system, unlike the theoretical one studied in the Analysis section, has certain transfer functions that are more or less fixed. Furthermore, in taking the derivative necessary for the predictions, new transfer functions must arise. Thus, what must be done for stability, what can be done to improve stability, and what can be done to improve the response are questions considered first.

Once a stable and reasonably fast system has been secured, the next question is that of its adequacy as a predictor system. In the examination of this question, first- and second-order prediction systems will be compared. The basis of comparison will be the distance by which the rockets miss a maneuvering target.

### Stability

As has been mentioned in the section on Analysis, the primary factor in achieving stability in the system is the removal of the ownship component of maneuvering acceleration ( $V_a \dot{\gamma}$ ) from the prediction equations before submitting them as commands to the airplane's autopilot and time servo. Figures 10 and 11 indicate the behavior of the system under changes in the amount of  $V_a \dot{\gamma}$  in the command. On the tests from which these time histories of  $V_a \dot{\gamma}$  were taken, the interceptor flew against a target initially 6,000 feet ahead. The interceptor speed was 1,000 feet per second; target speed was 800 feet per second. At 20 seconds to go (before predicted impact of rocket and target), the target pitched up at the rate of 0.06 radian per second, which corresponds to a maneuvering acceleration

of 1.5 g's, and held this heading change rate until the run was over. This sort of target maneuver will be referred to as a step target acceleration of 1.5 g's.

The time histories of figure 10 indicate that the presence in the commands of a component of ownship acceleration normal to the radar line-of-sight (the prediction equations are written in radar coordinates) acts in the sense of a negative feedback. The less its removal, the greater the feedback. The sequence of time histories in the figure shows that progressive removal of amounts of the feedback increases the effective forward gain of the airplane system as far as the first peak of the response is concerned. The period of the oscillations in figure 10(a) shows the effect of the interceptor-target geometry on the period of the system in this case. On the basis of the tests from which these time histories were taken, it appeared that the best response occurs if about 30 percent of the ownship acceleration (corresponding to  $K = 0.7$  in fig. 8(a)) is left in the elevation channel. With this amount of feedback, the response is as shown in figure 10(c).

During the runs from which the time histories of figure 10 were taken, as much ownship acceleration as possible was removed from the time channel. Leaving any ownship acceleration in the time channel has a deleterious effect on the stability of the system. Figure 11 shows a sequence of time histories of  $V_a \dot{\gamma}$  during runs with progressively less ownship acceleration remaining in the time channel (corresponding to changing the value of  $K$  from 0 to 1 in fig. 9(a)). In this run, 30 percent of the ownship acceleration component was left in the elevation channel. But this time, the effect on stability was more severe.

Adjustment of computer lags.— Once the basic stability of the system has been secured by proper removal of ownship accelerations, the choice of the various lags in the time and elevation computer loops can be investigated. The transfer functions of the differentiations govern the values of other lags to be inserted. The value of 1 second for the time constant of derivative process yielding  $\ddot{R}$  (shown in figs. 8 and 9) was chosen because the largest value of the effective numerator time constant,  $T/2$ , is 10 seconds. A lead-to-lag ratio of 10:1 is usually considered a reasonable compromise between response speed and induced noise. Attempts to vary this time constant as a function of  $T$  from 1 second to a small value not only led to considerable complexity, but also provided little success. The other terms in the command equations were put through lags to match them to the differentiated signal. In the time channel, the matched signals are  $R^2$ ,  $V_a \dot{\gamma} \sin E$ , and  $F \cos E$ . The range,  $R$ , varies slowly enough that the lag is unnecessary. In the elevation channel, the matched signals are  $V_a \dot{\gamma} \cos E$  and  $(F/T) \sin E$ . As shown in figure 8(a), a time constant of 2 seconds proved to be a better choice for the latter quantity.

Elevation dead zone.- Test runs with the attack computer arranged as described above showed adequate stability against a step target acceleration. However, when the target did not maneuver, the interceptor had a tendency to wander, with an amplitude of normal acceleration which was small at long and short interceptor ranges and larger at intermediate ranges. Insertions of a small dead zone 2 ft/sec<sup>2</sup> wide in the elevation acceleration terms removed this tendency. The effect of the dead zone is a small uncertainty in the predicted normal relative velocity, corresponding to the noise level of the electronic computer elements as amplified by the process of differentiation. No such noise problem arose in the time channel. In fact, it was found possible to increase the gain of the acceleration term in this channel from  $T^2/2$  to  $T^2$ .

#### Miss Evaluation

After the various parts of the attack computer had been adjusted in the manner just described, it was desired to compare the performance of the second-order prediction system with that of the first-order system by means of the rocket miss. There are four series of tests in this evaluation program. In the first three series, the target airplane performed a step acceleration maneuver at some time during the run. In the last series, the target started pitching upward at some time during the run then, after various fixed intervals of time, resumed steady straight flight (at a constant angle of climb). Such a maneuver corresponds to a pulse target acceleration.

In the first and second series of tests, the target's normal acceleration change was set at 1, 1.5, and 2 g's (corresponding to heading-change rates of 0.04, 0.06, and 0.08 radian per second). In the first series, the limits that exist in the usual acceleration command system's elevation channel were removed. The results of this series then establishes the capability of the second-order system in comparison with the first-order system.

Figure 12 shows the results of this series of runs. The ordinate in the figure is the elevation miss per g of target maneuvering acceleration. The abscissa indicates the length of time the target maneuver lasted, from the time it began until the end of the run. The run ended 1.5 seconds after rocket firing time. Rocket firing time occurs when the time-to-go, given by the output of the time servo, is 1.5 seconds. The distance of the rockets from the target 1.5 seconds after firing time is taken to be the rocket miss, and is resolved into an elevation component and a time component of miss. Thus, an elevation component of miss plotted at  $t_m = 8$  seconds is the rocket miss after a run in which the target maneuvered during the last 8 seconds.

The misses resulting from runs against all three magnitudes of target acceleration were sufficiently proportional to the magnitude of the normal acceleration change that the results of each command system defined the single curve shown when the ordinate in the figure was used. Figure 12(a) shows the error to be expected of a first-order system. The improvement to be expected by using a second-order system is shown by comparison of the curves in figures 12(a) and (b). The initial rise in the curves, up to 1.5 seconds, is due to the distance the target can climb during the time the rockets are flying. A maneuver begun during this period has no effect on the interceptor, which has already fired its rockets. The miss curves keep rising during the time the interceptor becomes aware of the maneuver and begins to respond. The curves reach a maximum when the interceptor begins to outclimb the target. Since in the second-order system the acceleration commanded of the interceptor does not cease until the interceptor is headed to a rocket impact point predicted on the basis that the target will continue to maneuver at its present rate, the miss curve drops to a small value after about 5 seconds of maneuvering. In the first-order system (fig. 12(a)), however, since the interceptor tends to point to an impact point along the tangent to the target's flight path, the miss remains proportional to the rate at which this impact point is changing.

The effect of limiting.- Figure 13 illustrates the effect of limiting the interceptor's acceleration command. The limits used in these tests restricted the total acceleration of the interceptor to stay between  $+3g$  and  $-1g$ . Figure 13(a) shows that since the commanded acceleration of the first-order system is relatively mild, these limits do not affect the interceptor's performance until the target's acceleration approaches the limit magnitude. Since the interceptor cannot head off a target which has a maneuvering acceleration equal to the incremental acceleration allowed the interceptor, the miss increases with maneuver duration.

This same effect is noticeable in figure 13(b) for the case of the  $2g$  step target acceleration. For 1 and  $1.5g$ 's of target acceleration, the miss curves return more slowly toward zero under conditions of limited acceleration capability. If unlimited, in the  $1.5g$  case, the interceptor attempts to pull a maximum of  $7g$ 's when the maneuver begins at long range. This is a peak, however, which remains above the allowed incremental value of 2 for only about 1 second.

Effect of rocket speed.- It was noted in the discussion of figure 12 that the miss curves rose during the first 1.5 seconds because during this time of rocket flight the interceptor had no power to correct the rocket's flight path. Reducing this flight time, which corresponds to increasing the rocket average speed, reduces the time available for the target to evade the interceptor. Consequently, it reduces the misses for both first- and second-order systems, as indicated in figure 14. Since here, as in all the other tests, the value of  $F$ , the distance traveled by the rocket relative to the interceptor, is fixed at 1500 feet, a time of flight  $t_f = 0.75$  corresponds to an average rocket speed of 2000 feet per second

with respect to the interceptor;  $t_f = 1.00$  corresponds to an average rocket speed of 1500 feet per second. All the runs which established the curves shown were made against a 1.5g step target acceleration with no limit on the acceleration command.

Pulse maneuvers.- In the final series of tests, the interceptor flew against a pulse target acceleration. During these tests, the acceleration command was not limited, and the rocket flight time was restored to 1.5 seconds. Figure 15 compares results of the first- and second-order systems for pulse widths  $\Delta t = 4-1/3, 6-1/2,$  and  $8-2/3$  seconds. The curves of figure 12 are added to represent the limiting case of wide pulses ( $\Delta t \rightarrow \infty$ ). The curves in the figure indicate the trend with change in  $\Delta t$ . The new curves follow those for a step acceleration until the abscissa is about 1.5 seconds longer than the pulse width. This time duration is due to rocket flight time. The curves for the first-order system (fig. 15(a)) drop to about zero, as they should, since the target is not maneuvering for some time before the end of the run. After all, in this system, when the target stops accelerating, the interceptor has only to stop accelerating too, for under these conditions of no maneuver, its predicted impact point has stopped moving. In the second-order case, on the other hand (fig. 15(b)), the interceptor has developed a large lead angle on the target to bring it to the predicted point. Between the time the maneuver has stopped and the time the interceptor has corrected its heading to a new point, a sizable miss occurs. This miss is largest for the smallest pulse width because for this case the difference in heading can become largest for, although the interceptor predicts the same impact point as for maneuvers of longer duration, the target changes its heading least in the shortest maneuver. To a second-order system, a maneuver lasting in the neighborhood of 3 or 4 seconds is the most serious because the difference in heading can be made greatest. As  $\Delta t$  becomes smaller, the interceptor is given less time to reach its predicted heading. As  $\Delta t$  becomes longer, the target heading angle increases and the interceptor's remains constant.

On the basis of these studies, it is clearly advantageous for the interceptor to have a second-order command system unless the target is going to maneuver for less than, say, 5 seconds. For maneuvers lasting between 3 and 5 seconds, the second-order command system is disadvantageous. For maneuvering of shorter duration, either system seems equally good. If only one kind of interceptor command system were available, and the target became aware of the attack, then the strategy of the target would be obvious. If both types of system are available, and especially if an attack were mounted by more than one interceptor; the target would find itself in a more awkward position.



## SUMMARY OF RESULTS

Against steady maneuvers, the effectiveness of automatic interception with first-order prediction deteriorates. The deterioration is not substantially lessened by improvements in system response, whether of the airplane-autopilot loop, or radar tracking loop, or both. A reasonable set of command equations can be devised by which the interceptor effectiveness does not deteriorate in the presence of target maneuvers of steady turning rates. Great care, however, is required in mechanizing the command equations because the miss distance is quite sensitive to the accuracy of computation. It seems that normal accuracy requirements satisfy as far as the magnitudes of added signals are concerned. But extra care must be exercised to match relative time shifts of added signals.

Both interceptor prediction and command channels are important from a stability standpoint and from a terminal accuracy standpoint.

For stability, as much interceptor acceleration as possible must be removed from the time channel equation. To leave some interceptor acceleration in the elevation channel command equation is not harmful. This residue is equivalent to additional feedback and has the effect of reducing the channel gain and system response.

Limiting the acceleration of the attacker has little effect on the misses obtained by an attacker under first-order commands, up to target accelerations of the magnitude of the limits. It increases the misses obtained by an attacker under second-order commands, however. With the latter system, therefore, the limits should be set as wide as is consonant with structural and buffeting requirements.

Results indicate that, with first- and second-order commands, the accuracy of the system is generally improved the higher the average rocket speed.

Ames Research Center  
National Aeronautics and Space Administration  
Moffett Field, Calif., Aug. 22, 1958

## APPENDIX A

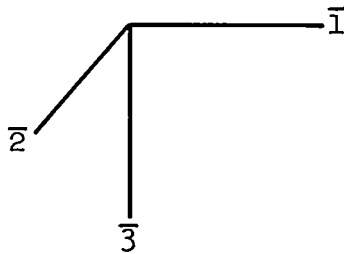
## DERIVATION OF SECOND-ORDER PREDICTION

## AND COMMAND EQUATIONS

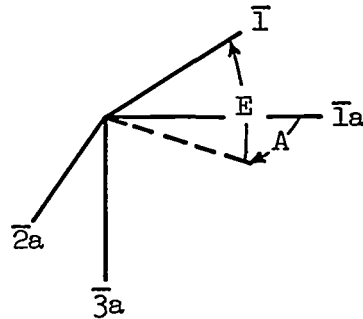
In the Analysis section of this report, the vector equation for miss has been given as  $\bar{M} + \bar{F} = \bar{R} + \dot{\bar{R}}T + \ddot{\bar{R}}T^2/2$ . This appendix contains first of all, the derivation of the expression for miss in radar coordinates of three dimensions. Then this triplet of equations is reduced to the pair used in the body of the report. Next, the two-dimensional expression for miss is derived in Cartesian coordinates. Finally, the two-dimensional equations of command are obtained.

## Three-Dimensional Prediction Equation

The radar coordinate system is defined by the triad of unit vectors shown with their orientation in sketch (d). The unit vector  $\bar{1}$  falls along the line-of-sight direction. The relationship between radar and interceptor coordinates is shown in sketch (e). The unit vector  $\bar{1}_a$  shown in this sketch defines the interceptor's longitudinal axis



Sketch (d)



Sketch (e)

The general vector expression for the time derivative of a vector  $\bar{R}$  in a rotating coordinate system is  $\dot{\bar{R}} = \frac{\partial}{\partial t} \bar{R} + \bar{\Omega} \times \bar{R}$ . The first term on the right expresses the change rate of the vector due to its explicit time dependence. The second term on the right expresses its change rate due to the instantaneous rotation rate of the coordinates in which it is given. Since in the present problem  $\bar{R} = R\bar{1}$  only,

$$\dot{\bar{R}} = \frac{d}{dt} \bar{R} = \bar{1} \frac{\partial R}{\partial t} + R\bar{\Omega} \times \bar{1} = \dot{R}\bar{1} + R(\Omega_3\bar{2} - \Omega_2\bar{3}) \quad (A1)$$

the time derivative operation can be performed on the vector  $\dot{\bar{R}} = \frac{\partial}{\partial t} \bar{R} + \bar{\Omega} \times \bar{R}$

$$\frac{d}{dt} \dot{\bar{R}} = \ddot{\bar{R}} = \frac{\partial^2}{\partial t^2} \bar{R} + \frac{\partial}{\partial t} (\bar{\Omega} \times \bar{R}) + \bar{\Omega} \times \frac{\partial}{\partial t} \bar{R} + \bar{\Omega} \times (\bar{\Omega} \times \bar{R}) \quad (A2)$$

now

$$\bar{\Omega} \times \frac{\partial}{\partial t} \bar{R} = \dot{R} (\Omega_3 \bar{2} - \Omega_2 \bar{3}) \quad (A3)$$

and

$$\bar{\Omega} \times (\bar{\Omega} \times \bar{R}) = -\bar{1} R (\Omega_2^2 + \Omega_3^2) + \bar{2} R \Omega_1 \Omega_2 + \bar{3} R \Omega_1 \Omega_3 \quad (A4)$$

Substituting by means of equations (A1), (A3), and (A4) into the expression for miss and separating the various components yield

$$M_1 = -F_1 + R + T \dot{R} + \frac{T^2}{2} \ddot{R} - \frac{T^2}{2} R (\Omega_2^2 + \Omega_3^2)$$

$$M_2 = -F_2 + T R \Omega_3 + \frac{T^2}{2} \frac{\partial}{\partial t} R \Omega_3 + \frac{T^2}{2} \dot{R} \Omega_3 + \frac{T^2}{2} R \Omega_1 \Omega_2$$

$$M_3 = -F_3 - T R \Omega_2 - \frac{T^2}{2} \frac{\partial}{\partial t} R \Omega_2 - \frac{T^2}{2} \dot{R} \Omega_2 + \frac{T^2}{2} R \Omega_1 \Omega_3$$

or

$$\left. \begin{aligned} M_1 &= -F_1 + R + T \left( 1 + \frac{T}{2} \frac{\partial}{\partial t} \right) \dot{R} - \frac{T^2}{2} R (\Omega_2^2 + \Omega_3^2) \\ M_2 &= -F_2 + \frac{T}{R} \left( 1 + \frac{T}{2} \frac{\partial}{\partial t} \right) R^2 \Omega_3 + \frac{T^2}{2} R \Omega_1 \Omega_2 \\ M_3 &= -F_3 - \frac{T}{R} \left( 1 + \frac{T}{2} \frac{\partial}{\partial t} \right) R^2 \Omega_2 + \frac{T^2}{2} R \Omega_1 \Omega_3 \end{aligned} \right\} \quad (A5)$$

The vector  $\bar{F}$  in these equations is the distance the rocket travels relative to the interceptor. It has been assumed in this report that  $\bar{F} = F \bar{1}_w$  only where  $\bar{1}_w$  is a unit vector along the interceptor's longitudinal wind axis. Under conditions of no sideslip,  $\bar{F}$  can be expressed in radar coordinates through the relationship

$$\begin{bmatrix} F_1 \\ F_2 \\ F_3 \end{bmatrix} = \begin{bmatrix} \cos E & 0 & -\sin E \\ 0 & 1 & 0 \\ \sin E & 0 & \cos E \end{bmatrix} \begin{bmatrix} \cos A & \sin A & 0 \\ -\sin A & \cos A & 0 \\ 0 & 0 & 1 \end{bmatrix} \begin{bmatrix} \cos \alpha & 0 & -\sin \alpha \\ 0 & 1 & 0 \\ \sin \alpha & 0 & \cos \alpha \end{bmatrix} \begin{bmatrix} F \\ 0 \\ 0 \end{bmatrix}$$

One obtains from this relationship the equations

$$F_1 = F(\cos E \cos A \cos \alpha - \sin E \sin \alpha)$$

$$F_2 = -F \sin A \cos \alpha$$

$$F_3 = F(\sin E \cos A \cos \alpha + \cos E \sin \alpha)$$

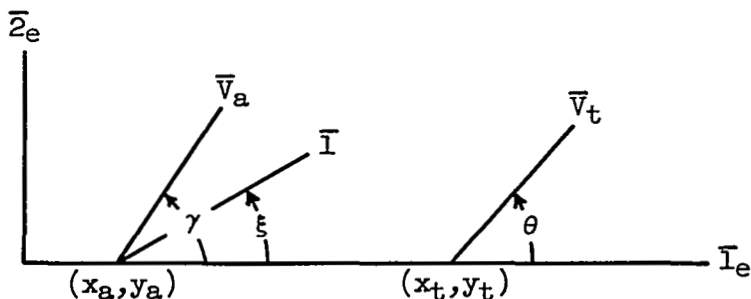
Substituting these expressions into equation (A5) and neglecting  $\alpha$ , one obtains

$$\left. \begin{aligned} M_1 &= R-F \cos A \cos E + T \left( 1 + \frac{T}{2} \frac{\partial}{\partial t} \right) \dot{R} - \frac{T^2}{2} R(\Omega_2^2 + \Omega_3^2) \\ M_2 &= F \sin A + \frac{T}{R} \left( 1 + \frac{T}{2} \frac{\partial}{\partial t} \right) R^2 \Omega_3 + \frac{T^2}{2} R \Omega_1 \Omega_2 \\ -M_3 &= F \sin E \cos A + \frac{T}{R} \left( 1 + \frac{T}{2} \frac{\partial}{\partial t} \right) R^2 \Omega_2 - \frac{T^2}{2} R \Omega_1 \Omega_3 \end{aligned} \right\} \quad (A6)$$

The reduction of these equations to two dimensions is easily accomplished by setting  $\Omega_3 = \Omega_1 = A = 0$ . It follows that  $M_2 = 0$  and

$$\left. \begin{aligned} M_1 &= R-F \cos E + T \left( 1 + \frac{T}{2} \frac{\partial}{\partial t} \right) \dot{R} - \frac{T^2}{2} R \Omega_2^2 \\ -M_3 &= F \sin E + \frac{T}{R} \left( 1 + \frac{T}{2} \frac{\partial}{\partial t} \right) R^2 \Omega_2 \end{aligned} \right\} \quad (A7)$$

Cartesian expressions in two dimensions.- The quantities to be employed in the miss equations in two-dimensional Cartesian form are illustrated in sketch (c).



Sketch (c)

As before,  $\bar{I}$  is a unit vector along the interceptor-to-target line of sight. The angle  $\xi$  is the radar space angle such that  $\dot{\xi} = \Omega$  which was written  $\Omega_2$  above. The coordinates of the interceptor and target are given by  $(x_a, y_a)$  and  $(x_t, y_t)$ , respectively. The vectors  $\bar{V}_a$  and  $\bar{V}_t$  define the headings of interceptor and target which are oriented in space by the angles  $\gamma$  and  $\theta$ , respectively. Finally,  $x_t - x_a = x$ ;  $y_t - y_a = y$ . It should be noted that, by the definition of  $\bar{R}$  and  $\bar{I}$ ,

$$\left. \begin{aligned} x &= R \cos \xi \\ y &= R \sin \xi \end{aligned} \right\} \quad (A8)$$

Starting from equation  $\ddot{\bar{M}} = -\ddot{\bar{F}} + \ddot{\bar{R}} + \ddot{\bar{R}}\dot{\bar{I}} + \ddot{\bar{R}}\frac{\pi^2}{2}$ , it is seen that

$$\left. \begin{aligned} M_{1e} &= -F_{1e} + x \cos \xi + y \sin \xi + T(\dot{x} \cos \xi + \dot{y} \sin \xi) + \frac{T^2}{2} (\ddot{x} \cos \xi + \ddot{y} \sin \xi) \\ M_{2e} &= -F_{2e} + y \cos \xi - x \sin \xi + T(\dot{y} \cos \xi - \dot{x} \sin \xi) + \frac{T^2}{2} (\ddot{y} \cos \xi - \ddot{x} \sin \xi) \\ &= -F_{2e} + T(\dot{y} \cos \xi - \dot{x} \sin \xi) + \frac{T^2}{2} (\ddot{y} \cos \xi - \ddot{x} \sin \xi) \end{aligned} \right\} \quad (A9)$$

That equations (A9) are equivalent to (A7) is shown by means of equations (A8).

Command equations.- The only source of acceleration in the problem is the heading changes of the two aircraft,  $V_a \dot{\gamma}$  and  $V_t \dot{\theta}$ . Hence  $\ddot{x}_a = -V_a \dot{\gamma} \sin \gamma$ ;  $\ddot{x}_t = -V_t \dot{\theta} \sin \theta$ ;  $\ddot{y}_a = V_a \dot{\gamma} \cos \gamma$ ;  $\ddot{y}_t = V_t \dot{\theta} \cos \theta$ .

Rewriting equations (A9) to illustrate this dependence, one obtains

$$\begin{aligned}
 M_{1e} &= -F_{1e} + x \cos \xi + y \sin \xi + T(\dot{x} \cos \xi + \dot{y} \sin \xi) + \\
 &\quad \frac{T^2}{2} [V_t \dot{\theta} (\sin \xi \cos \theta - \cos \xi \sin \theta) - V_a \dot{\gamma} (\cos \gamma \sin \xi - \sin \gamma \cos \xi)] \\
 &= -F_{1e} + x \cos \xi + y \sin \xi + T(\dot{x} \cos \xi + \dot{y} \sin \xi) + \\
 &\quad \frac{T^2}{2} [-V_t \dot{\theta} \sin(\theta - \xi) - V_a \dot{\gamma} \sin(\xi - \gamma)] \\
 M_{2e} &= -F_{2e} + T(\dot{y} \cos \xi - \dot{x} \sin \xi) + \frac{T^2}{2} [V_t \dot{\theta} \cos(\xi - \theta) - V_a \dot{\gamma} \cos(\xi - \gamma)]
 \end{aligned}
 \tag{A10}$$

From these equations, it is seen that in order to remove the effects of interceptor acceleration, the terms  $\frac{T^2}{2} V_a \dot{\gamma} \sin(\xi - \gamma)$  and  $\frac{T^2}{2} V_a \dot{\gamma} \cos(\xi - \gamma)$  are to be added to the miss equations. Returning to the form of equations as given in (A7) and realizing that  $\xi - \gamma = E + \alpha$  and  $M_{2e} = -M_3$ , one obtains the command equations

$$\begin{aligned}
 M_1 &= R - F \cos(E + \alpha) + T\dot{R} + \frac{T^2}{2} [\ddot{R} - R\Omega^2 + V_a \dot{\gamma} \sin(E + \alpha)] \\
 -M_3 &= F \sin(E + \alpha) + \frac{T}{R} \left( 1 + \frac{T}{2} \frac{\partial}{\partial t} \right) R^2 \Omega + \frac{T^2}{2} V_a \dot{\gamma} \cos(E + \alpha)
 \end{aligned}
 \tag{A11}$$

The inclusion of  $\alpha$  in the interceptor acceleration terms for the command equations is undesirable from a practical standpoint. Since it has also proved unnecessary, it was omitted in the simulation used in the present study.

## APPENDIX B

## DESCRIPTION OF THE EVALUATION OF MISS

Since the miss vector in this report is the separation between the rocket and target at some fixed time, namely 1.5 seconds after firing, the miss can be expressed in the following way

$$\bar{M} = \int_{t_1}^{t_2} (\bar{V}_t - \bar{V}) dt + \bar{M}_{t_1} \quad (B1)$$

In this expression,  $\bar{V}$  is the interceptor velocity plus the velocity of the rocket with respect to the interceptor:  $\bar{V} = \bar{V}_a + \bar{V}_m$ . The equation (B1) simply states that to calculate the miss one follows the relative trajectory from some starting point until the desired time. Choosing  $t_f$ , the firing time, as the starting point

$$\bar{M} = \bar{R}_{t_f} + \int_{t_f}^{t_f+1.5} (\bar{V}_t - \bar{V}_a - \bar{V}_m) dt = \bar{R}_{t_f} - \bar{F} + \int_{t_f}^{t_f+1.5} (\bar{V}_t - \bar{V}_a) dt \quad (B2)$$

Equations (B2) indicate that miss is evaluated exactly 1.5 seconds after the rocket has been fired, and that the rocket has such an average speed relative to the interceptor that its time integral over this interval is  $\bar{F}$ .

Since the rocket is assumed to fly along a straight line tangent to the interceptor's flight path at the instant of firing, it is convenient to express equations (B2) in the coordinates of the interceptor's wind system at firing time. Following the notation indicated in sketch (c) (and recalling that  $\xi - \gamma = E + \alpha$ ), and calling the unit wind coordinate vectors,  $\bar{1}_w$ ,  $\bar{2}_w$ ,  $\bar{3}_w$  with their usual orientation we find

$$\left. \begin{aligned} M_{1w} &= R_{t_f} \cos(E + \alpha) - \bar{F} + \int_{t_f}^{t_f+1.5} [V_t \cos(\gamma - \theta) - V_a] dt \\ M_{3w} &= -R_{t_f} \sin(E + \alpha) - \int_{t_f}^{t_f+1.5} [V_t \sin(\gamma - \theta)] dt \end{aligned} \right\} \quad (B3)$$

The only time-varying quantity in equation (B3) is the angle  $\theta$ .

Because of lack of analog equipment, the computation of miss components was done by hand. When  $T$ , the predicted time-to-go in the time

channel, decreased to 1.5 seconds, a pair of integrators began integrating the integrands in equations (B3). Except for the angle  $\theta$  which continued the target maneuver, and the integrations, the computer quantities were frozen. After exactly 1.5 seconds the integrators and  $\theta$  were frozen. The quantities of interest were then read.



## REFERENCES

1. Turner, Howard L., Triplett, William C., and White, John S.: A Flight and Analog Computer Study of Some Stabilization and Command Networks for an Automatically Controlled Interceptor During the Final Attack Phase. NACA RM A54J14, 1955.
2. Triplett, William C., McLean, John D., and White, John S.: The Influence of Imperfect Radar Space Stabilization on the Final Attack Phase of an Automatic Interceptor System. NACA RM A56K19, 1957.
3. Triplett, William C., and Hom, Francis W. K.: Flight Tests of an Automatic Interceptor System With a Tracking Radar Modified to Minimize the Interaction Between Antenna and Interceptor Motions. NACA RM A57D09, 1957.
4. Triplett, William C.: The Effects of a Modified Roll-Command System on the Flight Path Stability and Tracking Accuracy of an Automatic Interceptor. NACA RM A57L11a, 1958.
5. Woodling, C. H., and Gates, Ordway B., Jr.: Theoretical Analysis of the Longitudinal Behavior of an Automatically Controlled Supersonic Interceptor During the Attack Phase Against Maneuvering and Non-maneuvering Targets. NACA RM L55G18, 1955.
6. Anon.: Final Report Phase I Development of a Control Surface Tie-In Subsystem for the E-3/F-86D Weapon System. Res. and Dev. Labs., Hughes Aircraft Co., 28 Aug. 1953.

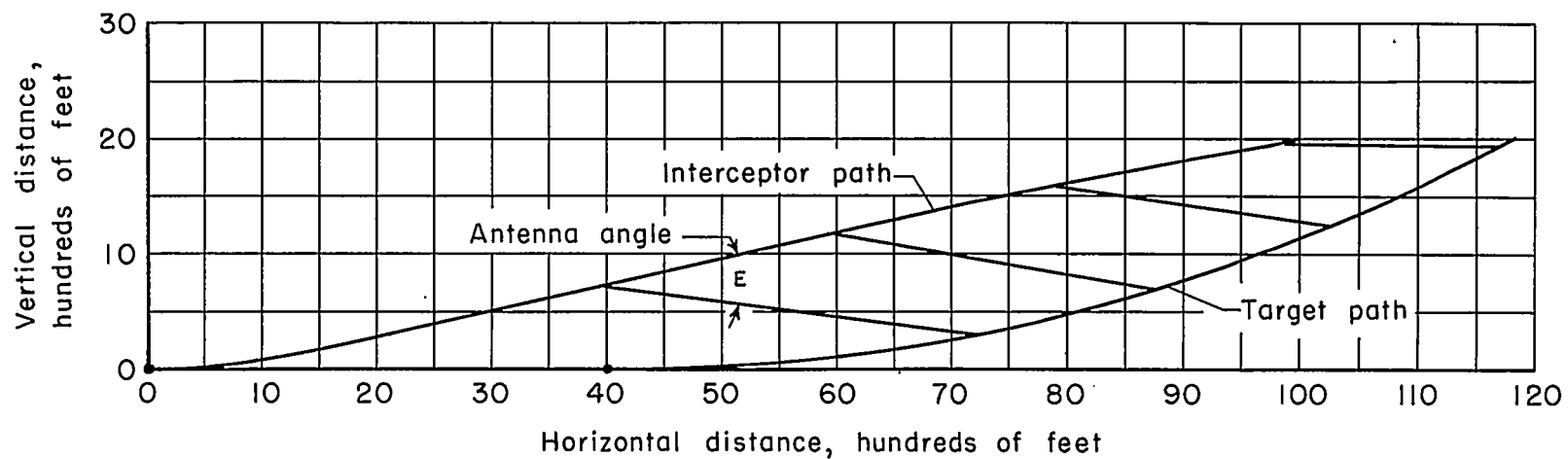
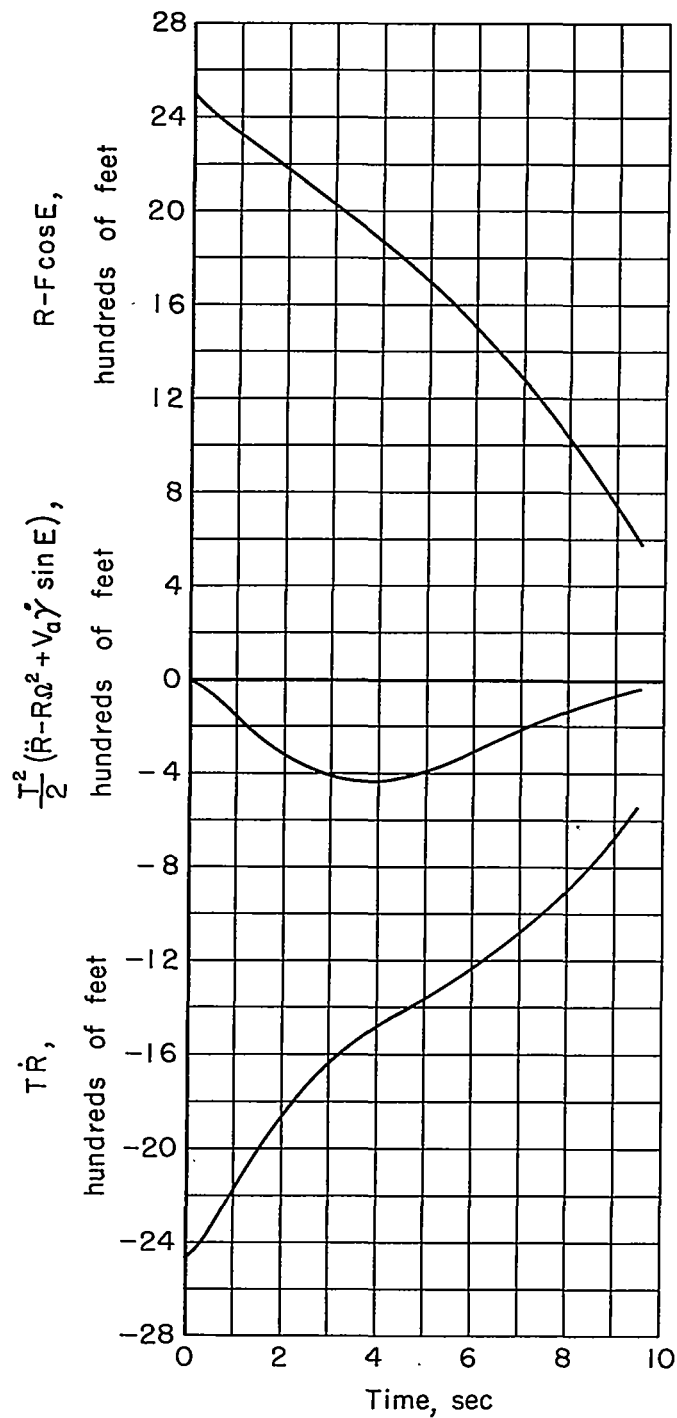
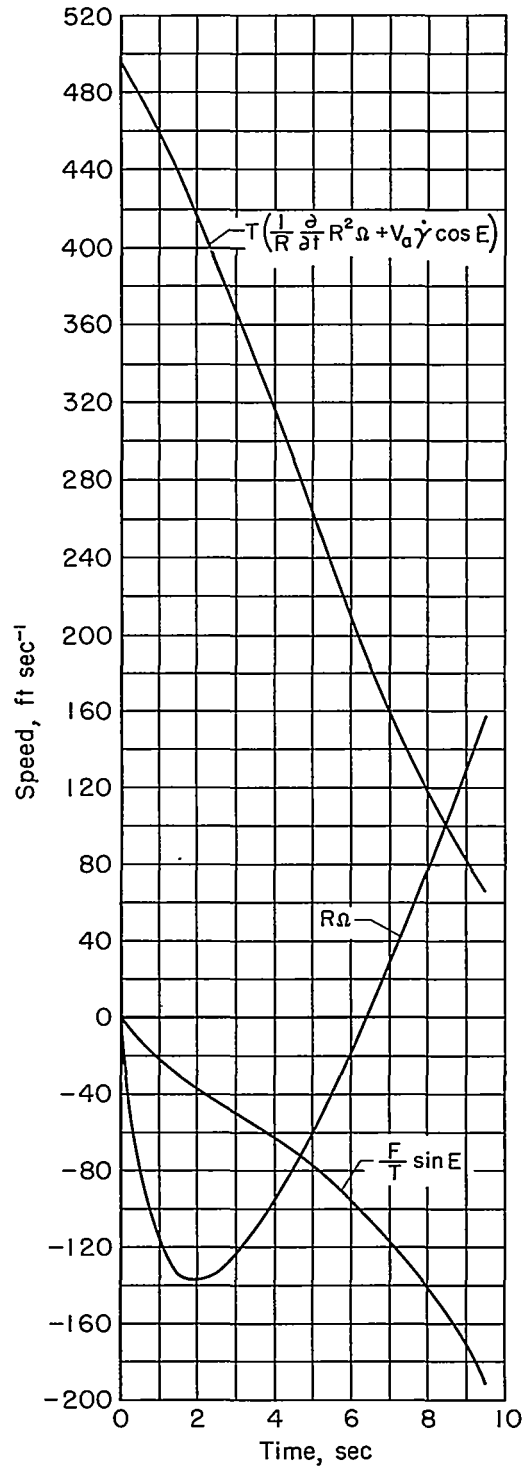


Figure 1.- Trajectory of interceptor with second-order command against a target performing a constant  $g$  pull-up maneuver.



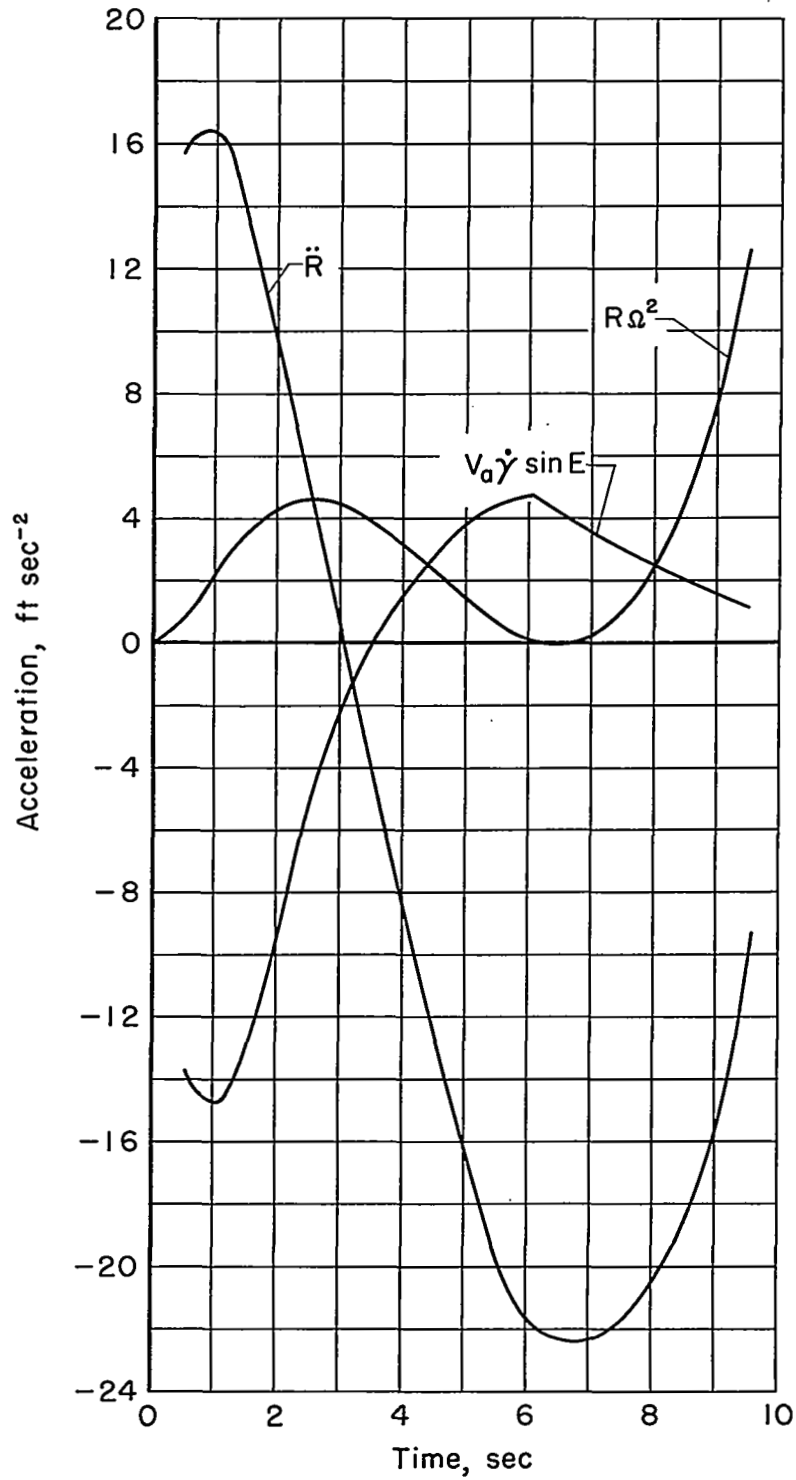
(a) Time channel terms.

Figure 2.- Time histories of terms of the second-order commands during the trajectory of figure 1.



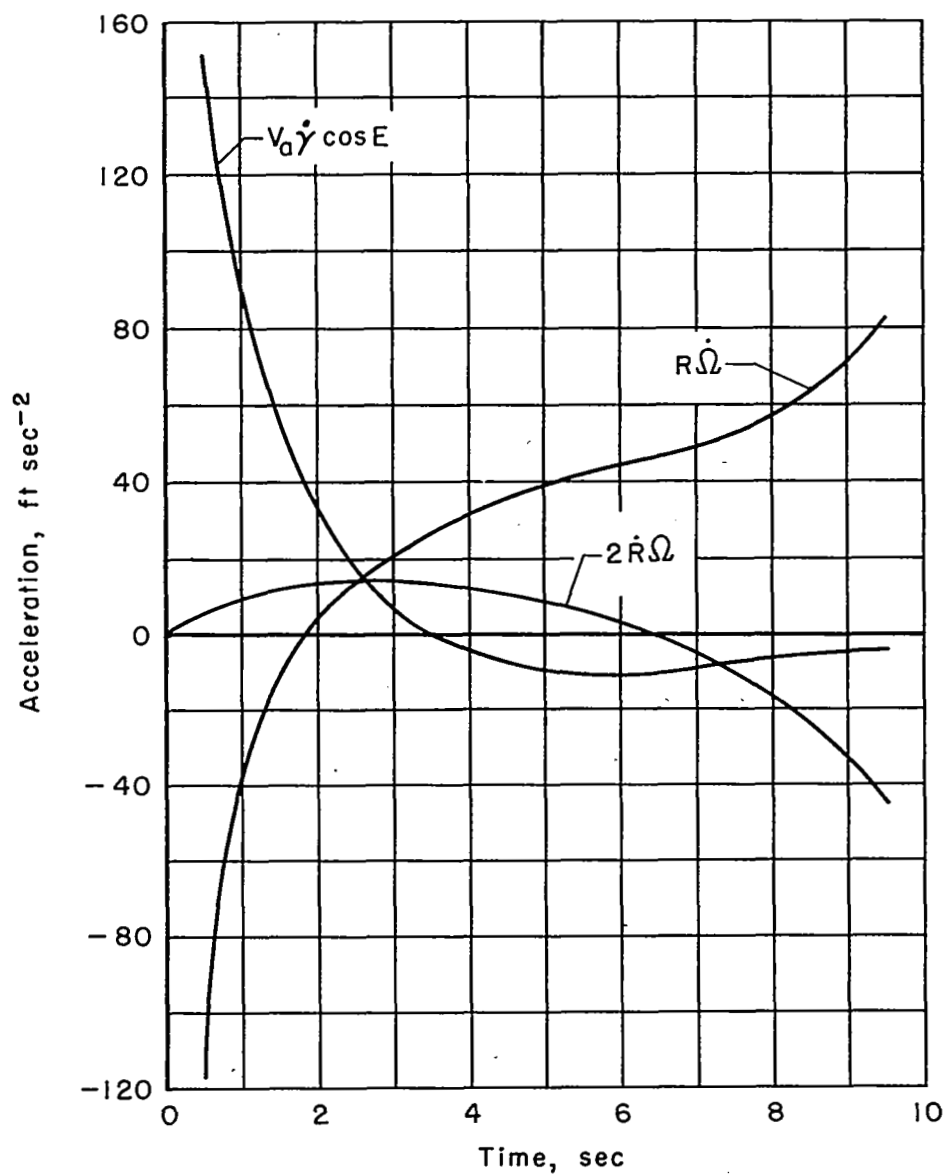
(b) Elevation channel terms.

Figure 2.- Continued.



(c) Acceleration term components in time channel.

Figure 2.- Continued.



(d) Acceleration term components in elevation channel.

Figure 2.- Concluded.

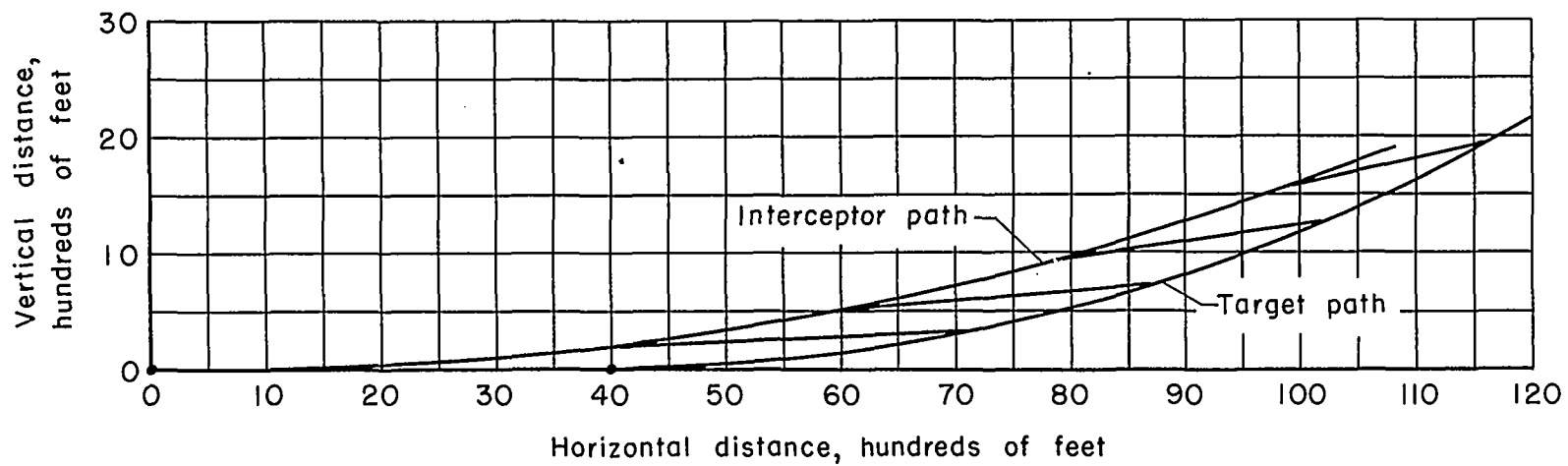
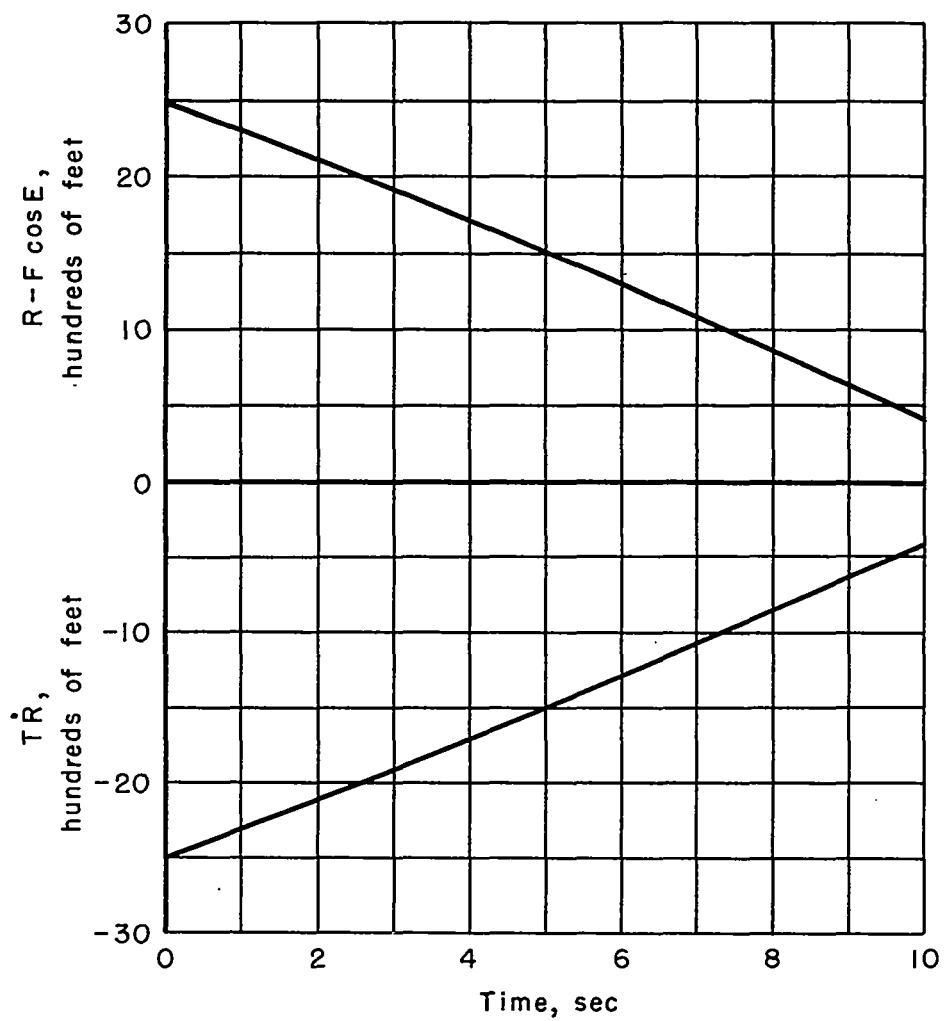


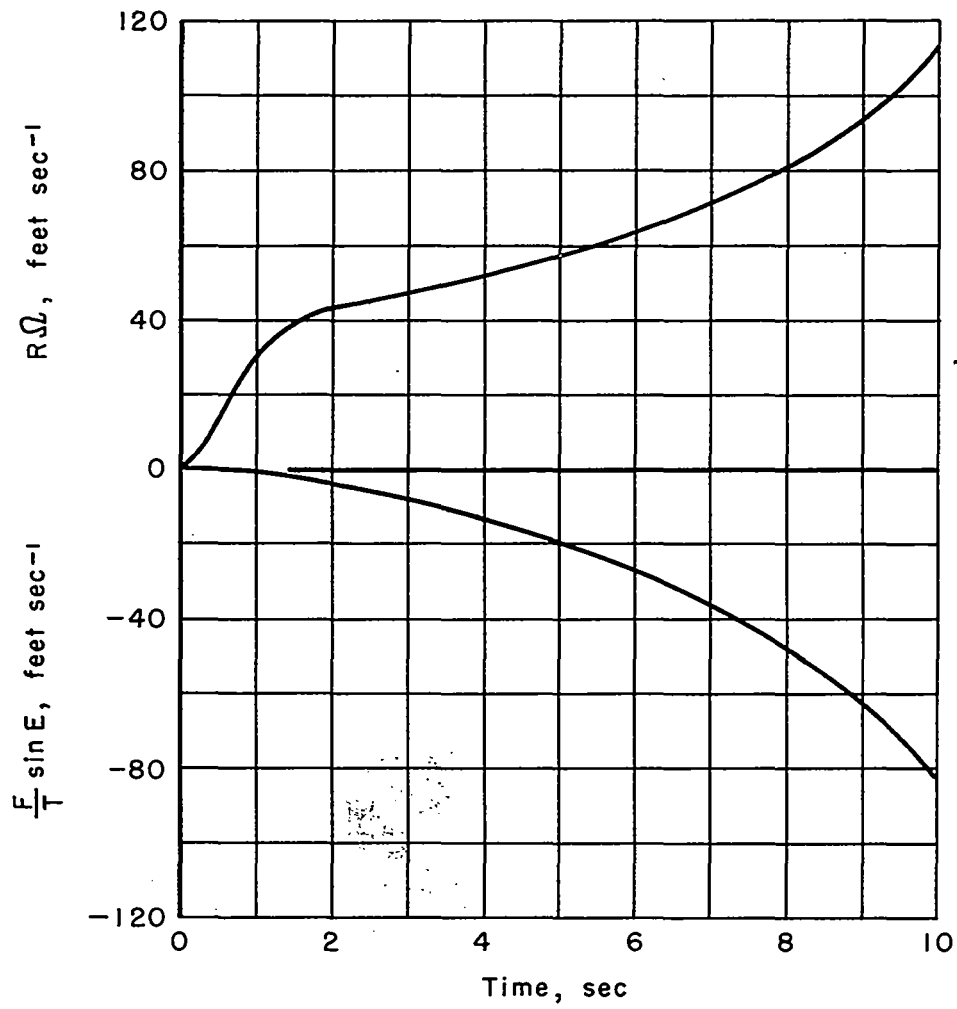
Figure 3.- Trajectory of interceptor with first-order command against a target performing a constant  $g$  pull-up maneuver.



(a) Time channel terms.

Figure 4.- Time histories of terms of first-order commands during the trajectory of figure 3.





(b) Elevation channel terms.

Figure 4.- Concluded.

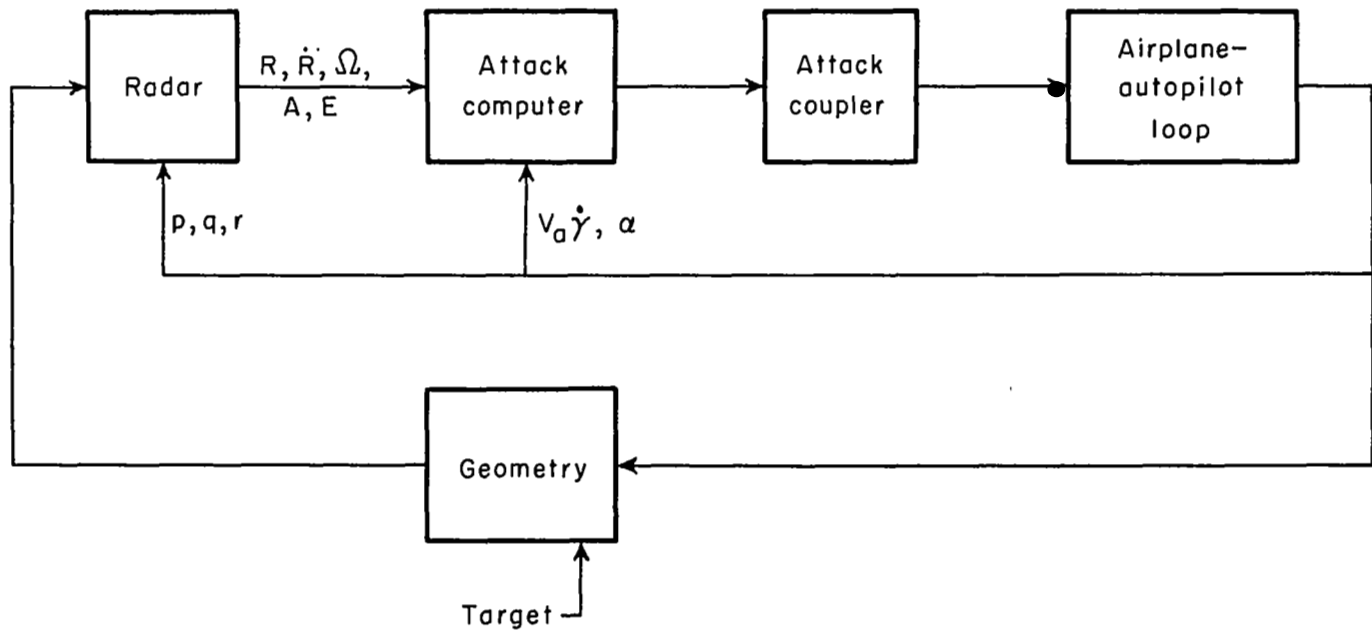
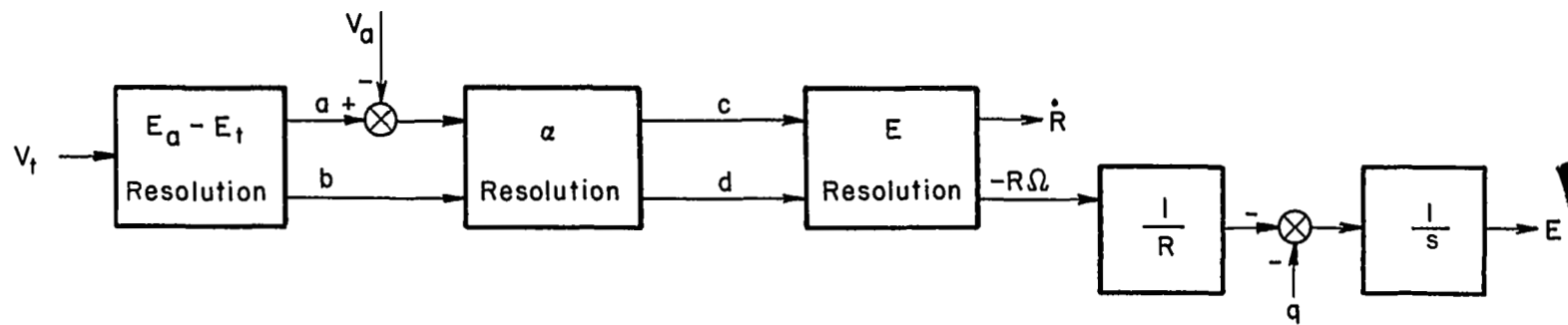


Figure 5.- Simplified block diagram of automatic interceptor system.



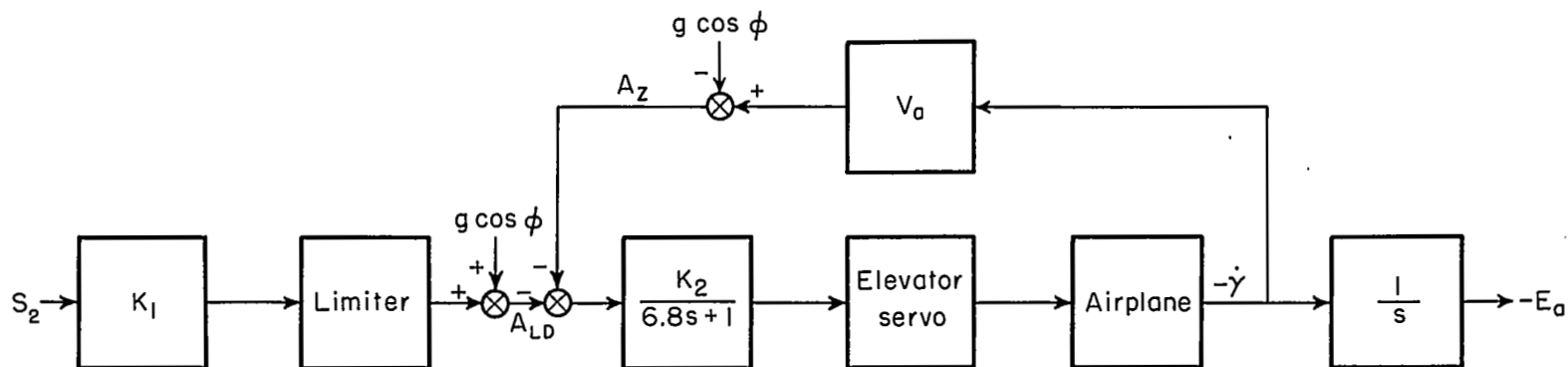
$$a = V_t \cos(E_a - E_t)$$

$$b = V_t \sin(E_a - E_t)$$

$$c = V_t \cos(E_a - E_t + \alpha) - V_a \cos \alpha$$

$$d = V_t \sin(E_a - E_t + \alpha) - V_a \sin \alpha$$

Figure 6.- Schematic block diagram of attack geometry.



$$K_1 = 1 \text{ ft sec}^{-2} / \text{ft sec}^{-1}$$

$$K_2 = .0046 \text{ radian} / \text{ft sec}^{-2}$$

$$V_d = 1000 \text{ ft sec}^{-1}$$

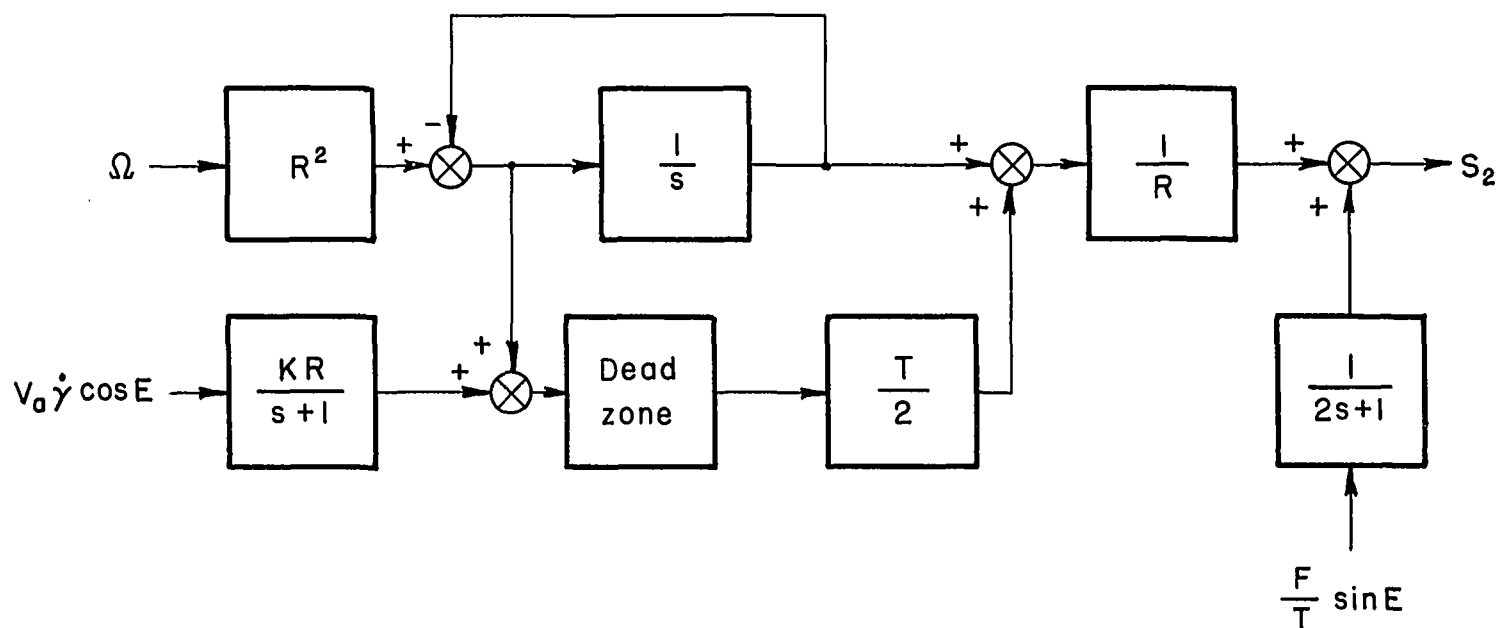
$$\text{Elevator servo transfer function: } \frac{1 \text{ radian/radian}}{.00625s^2 + .079s + 1}$$

$A_{LD}$  = Commanded acceleration

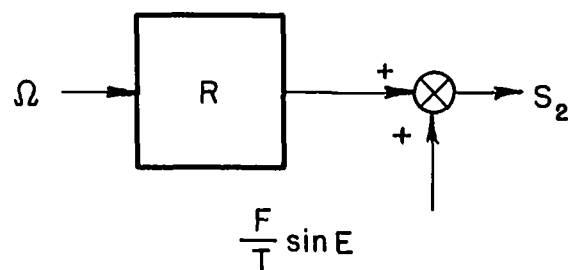
$$\text{Airplane transfer function: } \frac{1.768 \text{ radian sec}^{-1} / \text{radian}}{.0437s^2 + .0979s + 1}$$

$A_z$  = Measured acceleration

Figure 7.- Block diagram of attack coupler and airplane-autopilot loop.

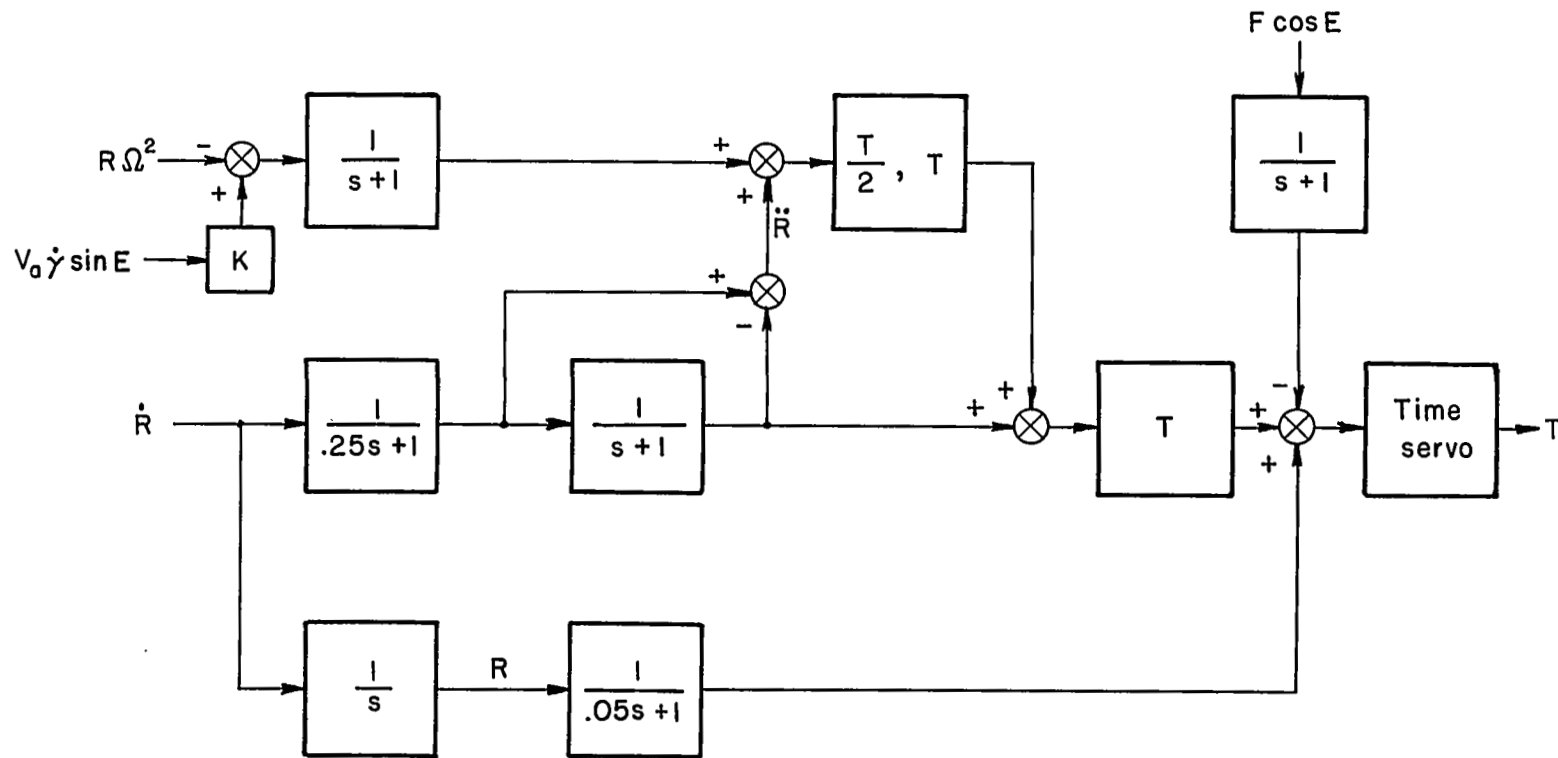


(a) Elevation channel of second-order command system.



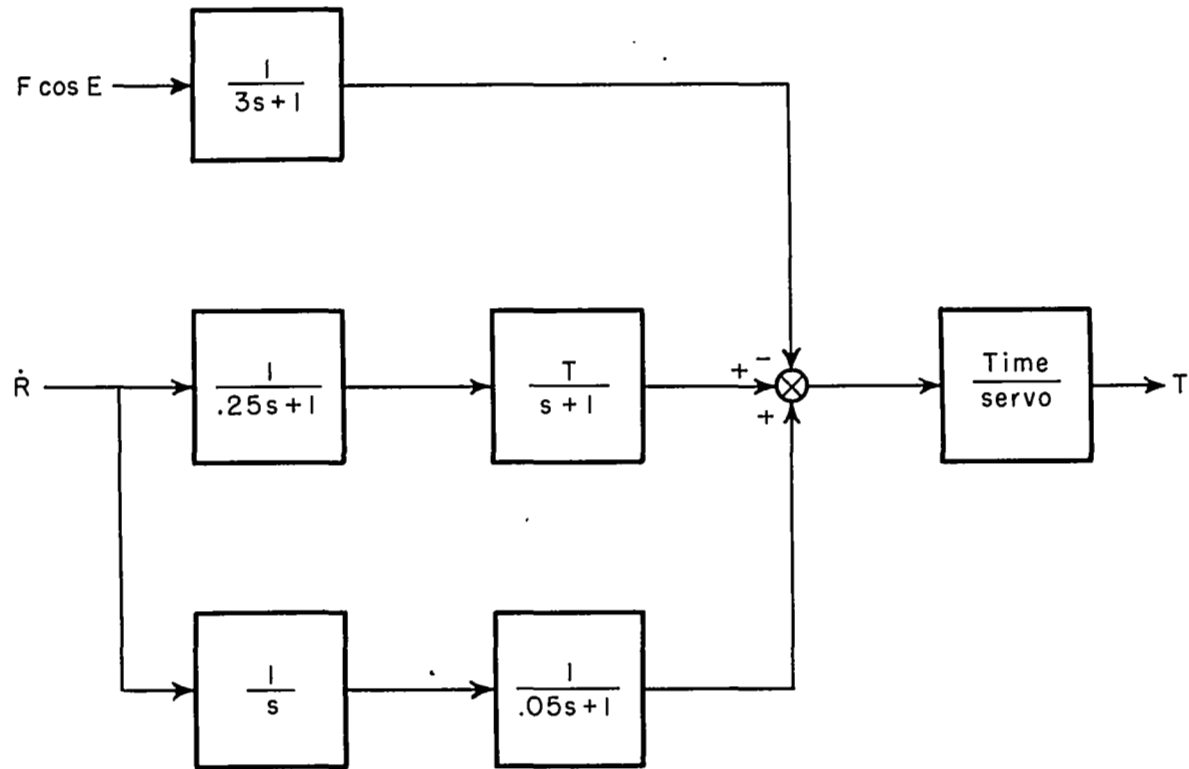
(b) Elevation channel of first-order command system.

Figure 8.- Block diagrams of elevation channel of attack computers for first- and second-order command systems.



(a) Time channel of second-order command system.

Figure 9.- Block diagrams of time channel of attack computer for first- and second-order command systems.



(b) Time channel of first-order command system.

Figure 9.- Concluded.

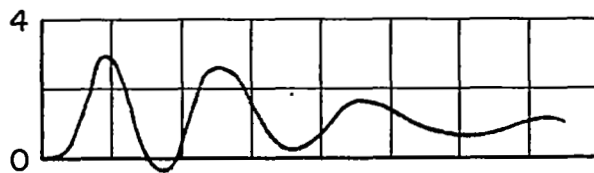
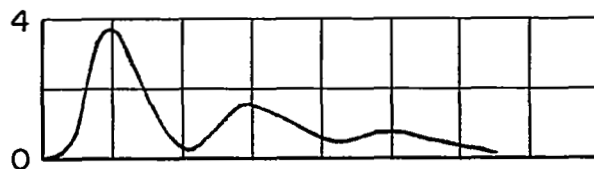
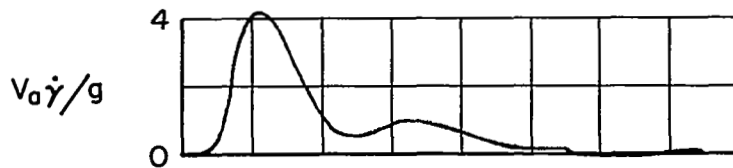
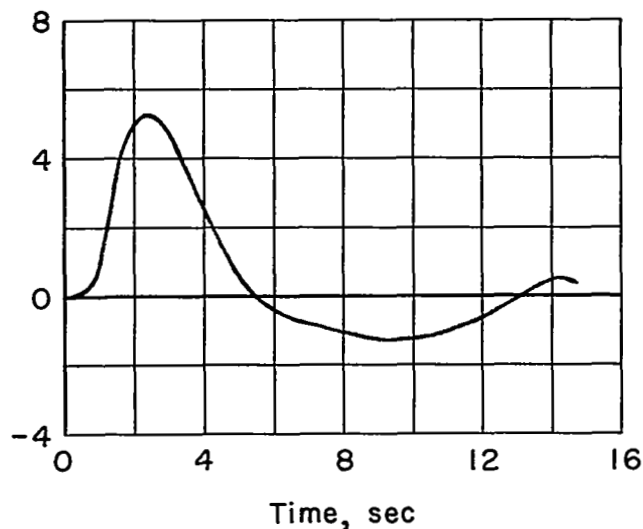
(a) No  $V_a \dot{\gamma} \cos E$  removed.(b) 50 percent  $V_a \dot{\gamma} \cos E$  removed.(c) 70 percent  $V_a \dot{\gamma} \cos E$  removed.(d) 100 percent  $V_a \dot{\gamma} \cos E$  removed.

Figure 10.- Time histories of interceptor maneuvering acceleration in response to a 1.5g steady target maneuver, illustrating the effect of removing ownship motion from the second-order elevation command, with all ownship motion removed from the time channel.



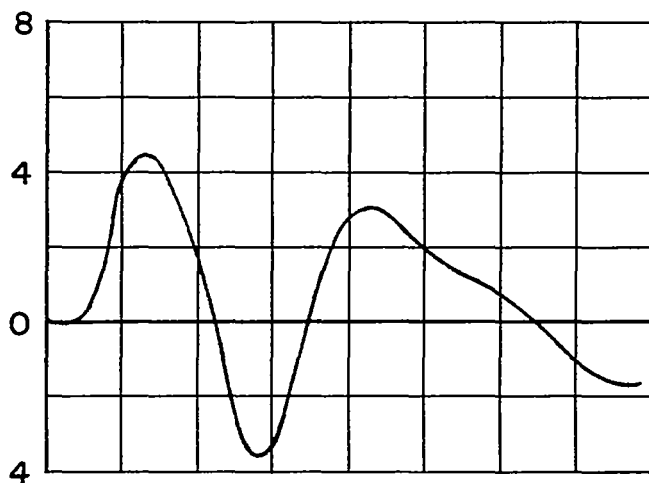
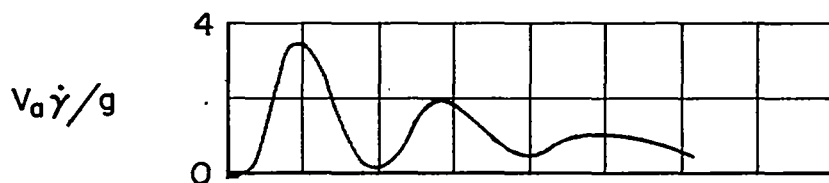
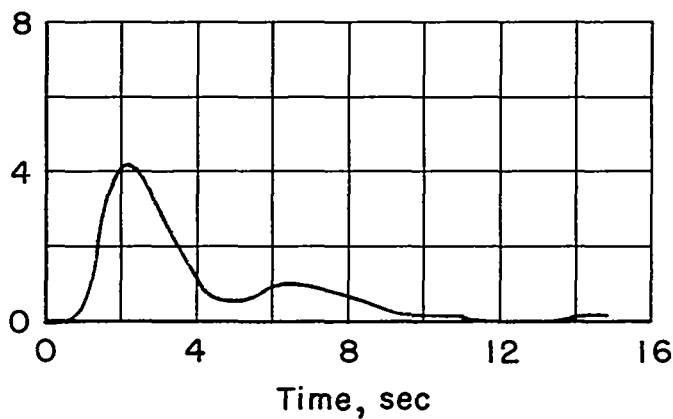
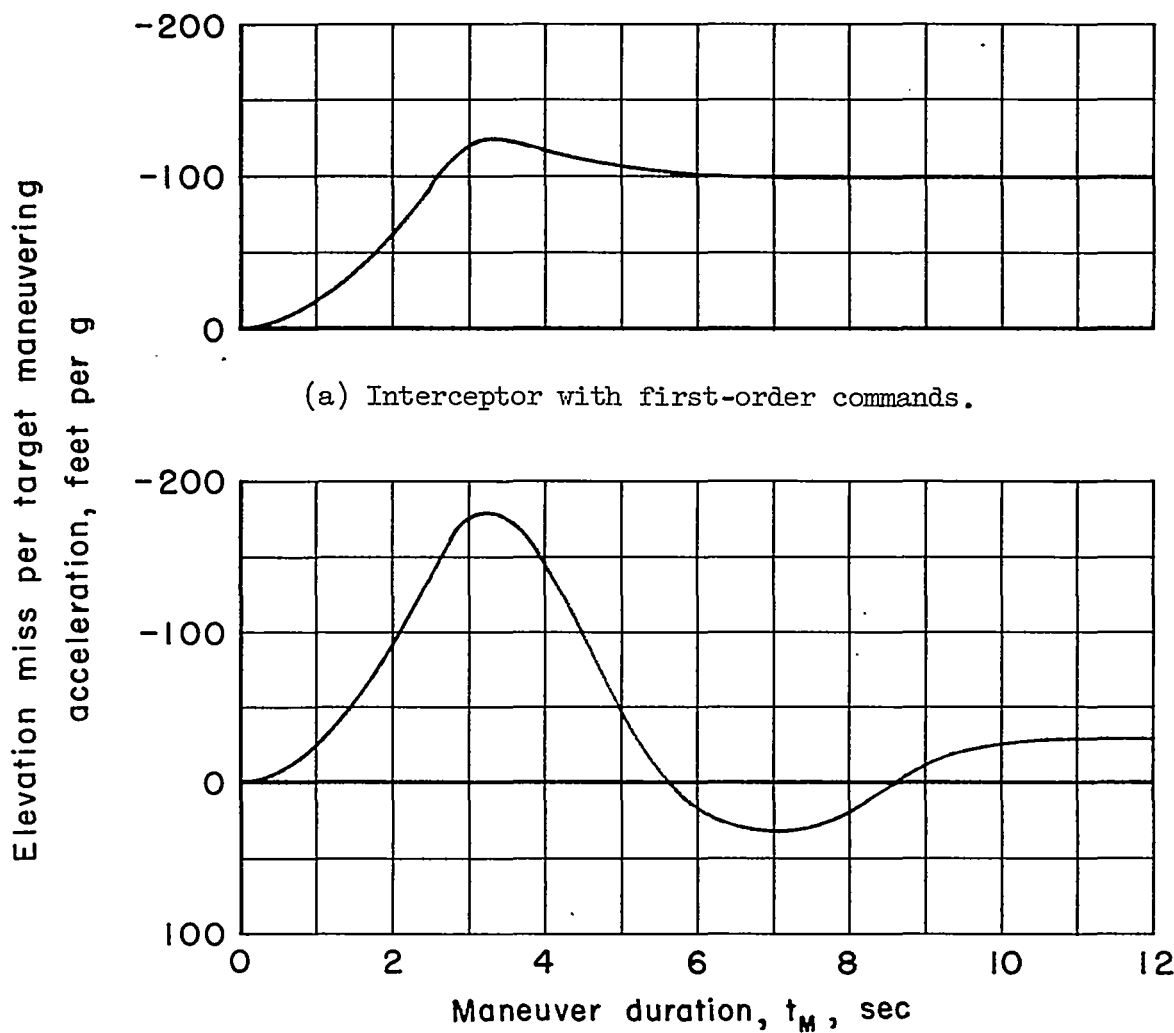
(a) No  $V_a \dot{\gamma} \sin E$  removed.(b) 50 percent  $V_a \dot{\gamma} \sin E$  removed.(c) 100 percent  $V_a \dot{\gamma} \sin E$  removed.

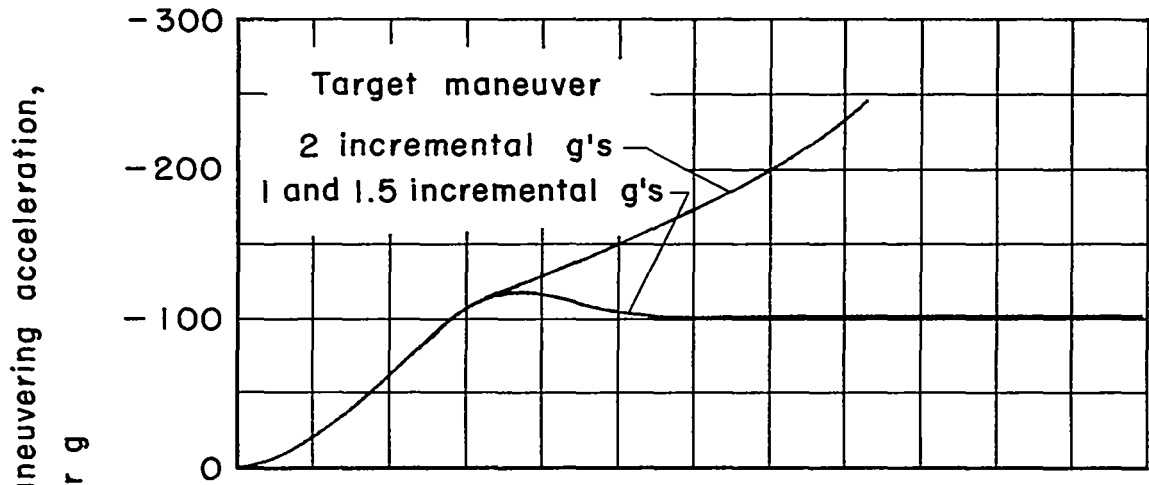
Figure 11.- Time histories of interceptor maneuvering acceleration in response to a 1.5g target maneuver, illustrating the effect of removing ownship motion from the second-order time channel, with 70 percent ownship motion removed from the elevation command.



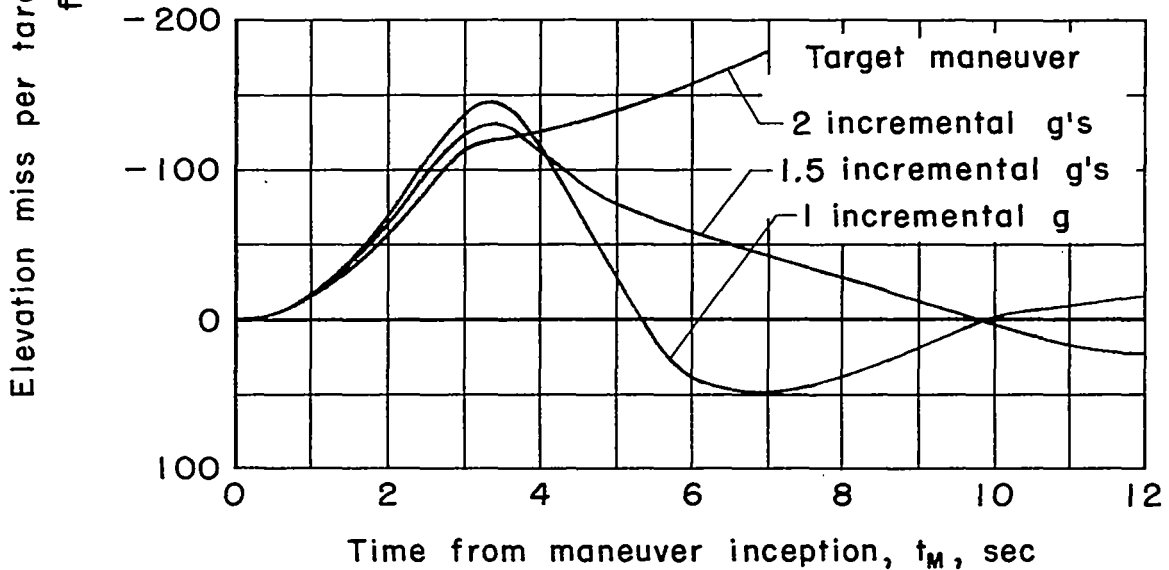
(a) Interceptor with first-order commands.

(b) Interceptor with second-order commands.

Figure 12.- Comparison of misses resulting from automatic interception with first- and second-order commands against a target maneuvering in a steady  $g$  turn. Interceptor acceleration capability not limited.

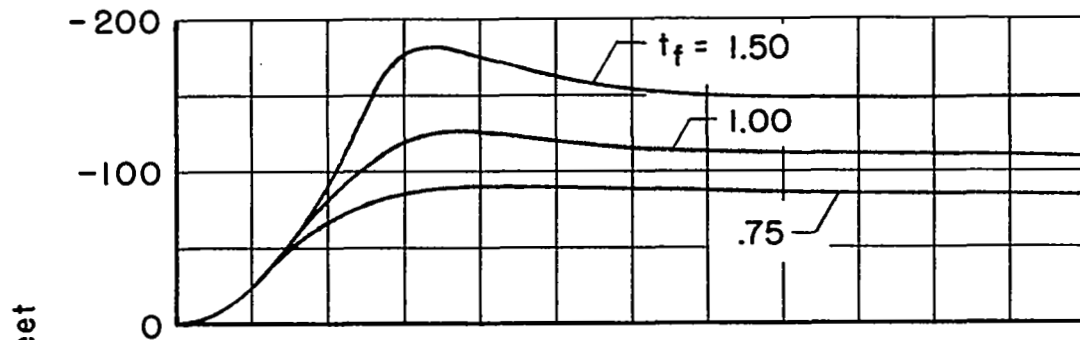


(a) Interceptor with first-order commands.

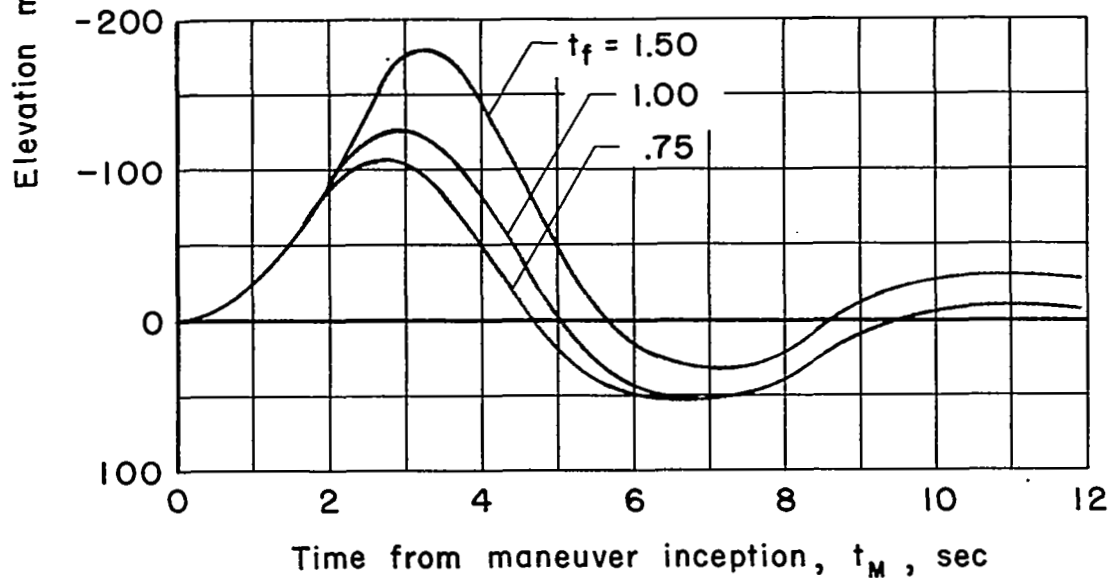


(b) Interceptor with second-order commands.

Figure 13.- Comparison of misses resulting from automatic interception with first- and second-order commands against a target maneuvering in a steady  $g$  turn. Interceptor acceleration capability limited.

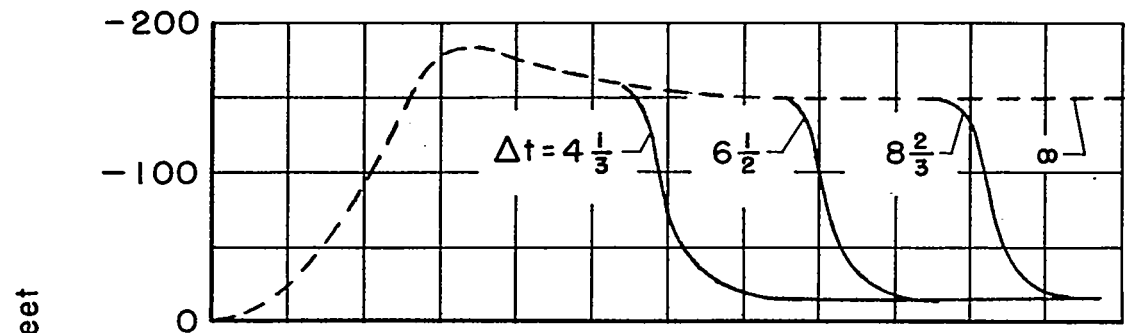


(a) Interceptor with first-order commands.

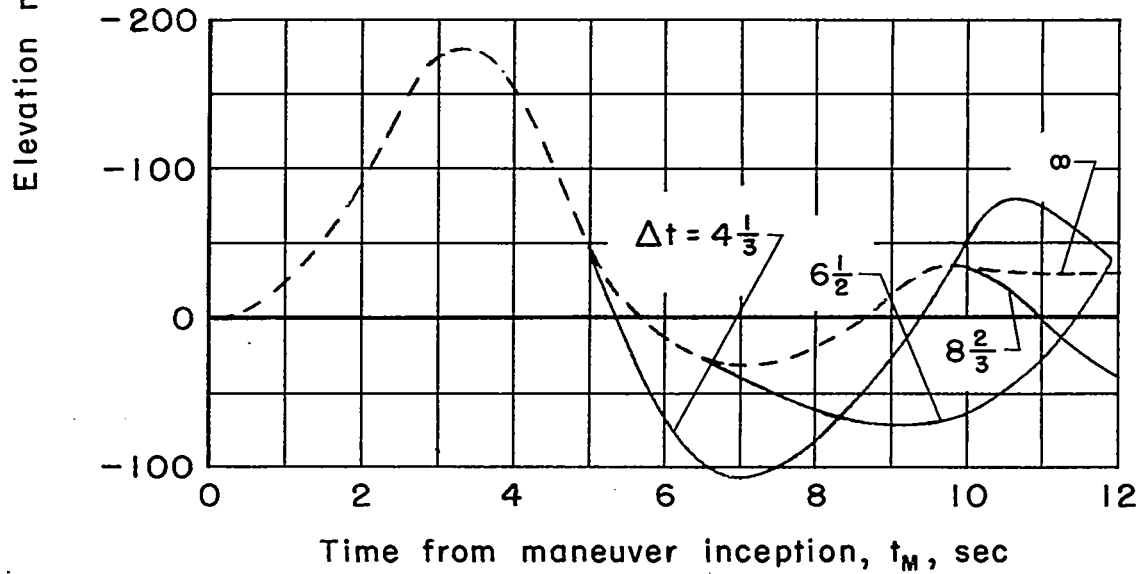


(b) Interceptor with second-order commands.

Figure 14.- Comparison of misses resulting from automatic interception with first- and second-order commands against a target maneuvering in a steady  $g$  turn for various rocket times of flight.



(a) Interceptor with first-order commands.



(b) Interceptor with second-order commands.

Figure 15.- Comparison of misses resulting from automatic interception with first- and second-order commands against a target maneuvering with 1.5 g's acceleration for various durations of time.